Biosensors and Bioelectronics 148 (2020) 111833

Contents lists available at ScienceDirect

Biosensors and Bioelectronics

journal homepage: http://www.elsevier.com/locate/bios

Optical and electrochemical-based nano-aptasensing approaches for the detection of circulating tumor cells (CTCs)

Hossein Safarpour [a], Sadegh Dehghani [b], Rahim Nosrati [c,d], Nozhat Zebardast [c], Mona Alibolandi [e], Ahad Mokhtarzadeh [f,**], Mohammad Ramezani [e,**]

[a] Cellular and Molecular Research Center, Birjand University of Medical Sciences, Birjand, Iran
[b] Department of Medical Biotechnology, Faculty of Medicine, Mashhad University of Medical Sciences, Mashhad, Iran
[c] Cellular and Molecular Research Center, School of Medicine, Guilan University of Medical Sciences, Rasht, Iran
[d] Department of Pharmaceutical Biotechnology, School of Pharmacy, Mashhad University of Medical Sciences, Mashhad, Iran
[e] Pharmaceutical Research Center, Pharmaceutical Technology Institute, Mashhad University of Medical Sciences, Mashhad, Iran
[f] Immunology Research Center, Tabriz University of Medical Sciences, Tabriz, Iran

ARTICLE INFO

Keywords:
Circulating tumor cells (CTCs)
Aptamer
Aptasensor
Biosensor
Nanoparticle
Cancer

ABSTRACT

More recently, detection of circulating tumor cells (CTCs) has been considered as an appealing prognostic and diagnostic approach for cancer patients. CTCs as a type of tumor-derived cells are secreted by the tumor and released into the blood circulation. Since the migration of CTCs is an early event in cancer progression, patients who still have tumor-free lymph nodes have to be well examined for the CTCs presence in their blood circulation. Nowadays, there is a broad range of detection methods available to identify CTCs. As artificial RNA oligonucleotides or single-stranded DNA with receptor and catalytic characteristics, aptamers have been standing out, owing to their target-induced conformational modifications, elevated stability, and target specificity to be implemented in biosensing techniques. To date, several sensitivity-enhancement methods alongside smart nanomaterials have been used for the creation of new aptasensors to address the limit of detection (LOD), and improve the sensitivity of numerous analyte identification methods. The present review article supports a focused overview of the recent studies in the identification and quantitative determination of CTCs by aptamer-based biosensors and nanobiosensors.

1. Introduction

Globally, cancer stays among the most widely cause of death due to challenges arising in the diagnosis and clinical management of cancer (Bray et al., 2018; Siegel et al., 2018). Recently, the effective employment of cancer diagnosis approaches, for early detection and developments of novel efficient therapeutic strategies have significantly decreased cancer mortality (Smith et al., 2018). However, patients with metastatic cancer remain incurable if the diagnosis is not performed efficiently and on time.

In this regard, circulating tumor cells (CTCs) are an important signature of tumor metastasis (Micalizzi et al., 2017). CTCs exist as a single or cluster of tumor cells that are secreted from the tumor tissue and released into the blood and lymph node circulation. Migration of CTCs is an early event in cancer progression, thus CTCs detection is critical in early diagnosis of asymptomatic tumors (Sundling and Lowe, 2019). Ideal strategies for the identification of CTCs not only allow the quantification of CTCs in the blood at the time of diagnosis, but also can be used as a tool for specific biomarker detection, if clinically validated (Schettini et al., 2019).

Given that the peripheral blood levels of CTCs are low, almost 1 cell per 10^5 to 10^7 mononuclear cells, their identification is absolutely difficult (Shen et al., 2017). Currently, several methods have been used to detect CTCs (Ignatiadis et al., 2015; Lou et al., 2018). Basically, depending on biological or physical properties of these methods, CTCs can be enriched positively or negatively. While immunoaffinity technologies are based on use of antibodies specifically binding to differentially expressed surface receptor of CTCs such as EpCAM-based enrichment (Alix-Panabières and Pantel, 2014), and capturing approaches relying on physical properties such as size, density, and electric

* Corresponding author. School of Pharmacy, Pharmaceutical Research Center, Mashhad University of Medical Sciences, P.O. Box: 91775-1365, Mashhad, Iran.
** Corresponding author.
E-mail addresses: mokhtarzadehah@tbzmed.ac.ir (A. Mokhtarzadeh), ramezanim@mums.ac.ir (M. Ramezani).

https://doi.org/10.1016/j.bios.2019.111833
Received 5 August 2019; Received in revised form 25 October 2019; Accepted 29 October 2019
Available online 1 November 2019

charge of the CTCs for the enrichment purposes (Arya et al., 2013). Due to missing tumor cells expressing specific cell-surface markers (EpCAM is mostly used), immunoaffinity-based methods may result in a high false-negative rate. Currently, only the CellSearch® platform (Veridex, Huntingdon Valley, PA), is FDA-approved for clinical use of enumeration in the setting of certain cancer types. However, the technique is time-consuming, requiring expensive equipment and antibody staining which limited the broad application of this technology (Kalinich et al., 2017). On the other hand, those methods recognizing CTCs through their physical properties are expected to have a higher false-positive rate due to trapping some blood cells (Li et al., 2018a). An additional limitation is the extended processing times for small sample volumes. For example, the CTC-iChip can process only 8 mL of whole blood per hour with an extra 1 h set-up time (Karabacak et al., 2014). In this way, the development of selective, extremely sensitive, rapid, cost-effective and label-free procedures for CTCs recognition in serum/blood is pivotal for early diagnosis of the metastatic state of cancer in the clinic.

Over the last few years, researchers have used a range of novel sensing platforms to detect CTCs (Shen et al., 2017). Biosensors have been significantly successful in detecting CTCs, owing to sensitivity, specificity, the low-cost and low limit of detection (LOD) of the target molecule. Biosensors, representing the technological counterpart of living senses, have found routine applications in medical diagnostics (Vigneshvar et al., 2016). The integration of nanoparticles (NPs) with extraordinary features in biosensing plan makes nano-biosensor platforms simpler, faster, more sensitive and hybrid with synergistic characteristics and actions (Li et al., 2018a; Pandey et al., 2008). NP complexes with various biorecognition elements such as polymers, peptide arrays, aptamers, oligonucleotides and antibodies provide various adaptable strategies for enhancing the efficacy of capturing constructs (Malekzad et al., 2017). Interestingly, aptamers are compatible with multiple platform designs in the growing field of biosensors contributing to the worldwide market for rapid medical diagnostic (Bruno, 2015). The global aptamers market is rapidly developing and predicted to reach US $244.93 million in 2020 (Malinee et al., 2019). In the current review, we summarized the results of the most recent studies in the field of aptamer-based biosensors (aptasensors) for CTCs identification.

2. Aptamers: the bioreceptor elements

Aptamers are RNA, single-stranded DNA (ssDNA), or altered nucleic acids with strong affinity for specific target binding. Aptamers generally exhibit defined structures due to their intrinsic propensity to form intramolecular base pairing of complementary nucleotides. They can fold into different types of secondary structures including stem, loop, bugle, pseudoknot, G-quadruplex and kissing hairpin (Mayer, 2009). Sequentially, the assembly of these secondary structures contribute to formation of unique three-dimensional (3D) structures that provide specific, high affinity binding to a wide variety of target molecules (Gelinas et al., 2016). Over the past few decades, many methods have been introduced to generate aptamers with greater efficiency and reliability. These include the systematic evolution of ligands by exponential Enrichment (SELEX) approach (Fig. 1) and its derivatives (Zhang et al., 2019b). The details of various types of SELEX methods was presented in the published review by Bayat and coworkers (Bayat et al., 2018). In a typical SELEX technique, a random DNA library containing 1014–1016 unique single-stranded oligonucleotide sequences is incubated with a target molecule of interest. The target-bound and unbound sequences are separated followed by PCR amplification of the target-bound sequences for using as inputs in the next round of selection. The repeated rounds of selection are performed to create a pool of aptamer sequences with high affinity for the target molecule. These aptamers will then be cloned and sequenced (Bayat et al., 2018; Zhang et al., 2019b).

A wide range of great chemical modifications and improvements to simplify the SELEX procedure or to generate aptamers with the desired modification include use of multiple targets to control specificity, changing the characteristics of the nucleic acid library, using different substrates for presentation of target molecules and varying the separation technique (Szeto et al., 2013). In addition to DNA libraries, RNA

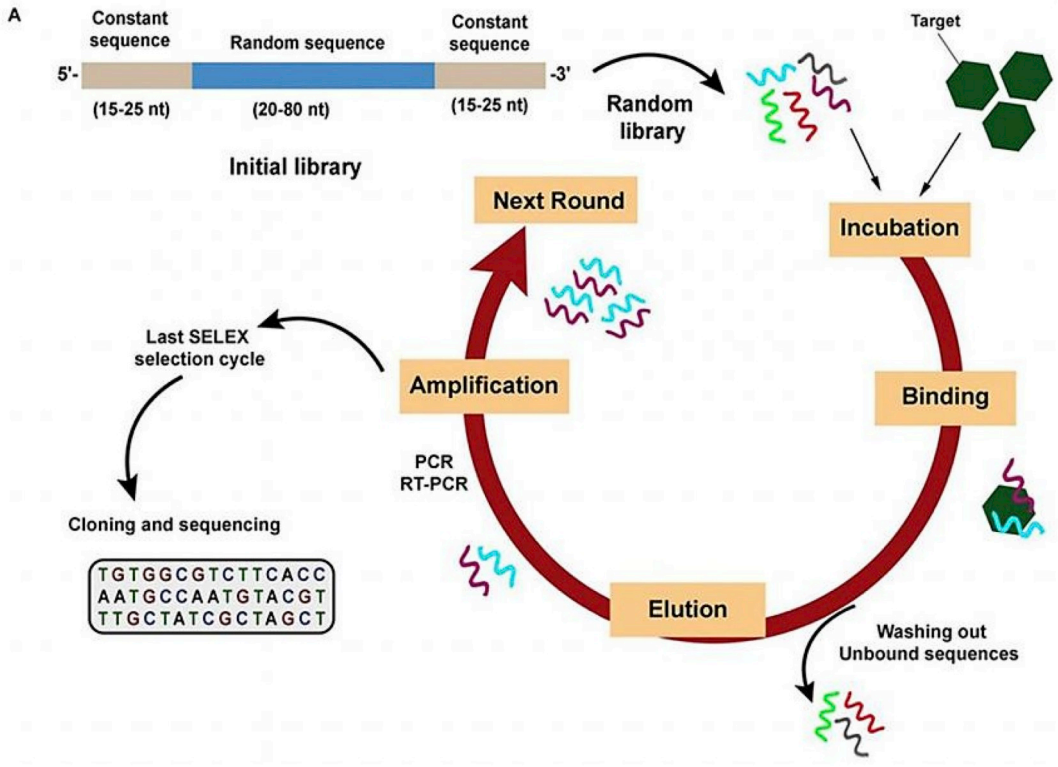

Fig. 1. Conventional SELEX for DNA aptamers generation. Reprinted with permission from (Bayat et al., 2018).

libraries have also been efficaciously introduced to SELEX (Zhou and Rossi, 2017). The main differences between RNA SELEX compared to DNA SELEX include the factors that protect RNA from the action of RNases, reverse transcription to amplifiable cDNA and subsequent transcription back to RNA. Consequently, a T7 RNA polymerase promoter placed at the 5′ end of primer is used for RNA SELEX (Vorobyeva et al., 2018).

Aside from comparable affinity and specificity, compared to antibodies, the advantages of aptamers include excellent flexibility and reversible denaturation of structure, easy modification with signal-generating molecules, no or rare immunogenicity, easily amplification by PCR, with no need for an *in vivo* immunization to obtain aptamers. In addition, due to high-throughput or automated *in vitro* isolation of aptamers, the overall development procedure is low cost, without batch-to-batch variation, more efficient and less time-consuming (Mokhtarzadeh et al., 2016; Scheller et al., 2014). On the basis of these great advantages, numerous isolated aptamers have been used as a sensing element in diagnostics (Aliakbarinodehi et al., 2017; Cengiz Ozalp et al., 2015), drug delivery (Chen et al., 2017; Mansouri et al., 2019; Yazdian-Robati et al., 2019), and theranostic tools, (therapy and diagnostic) (Mosafer et al., 2017; Sriramoju et al., 2015; Xiang et al., 2015) implementing the production of colorimetric, electrochemical and fluorescent signals (Dehghani et al., 2018).

3. Optical CTCs aptasensors and nano-aptasensors

Optical biosensors are a class of biosensors, in which optical detection is performed by exploiting the interaction of the optical field with a biorecognition element e.g. antigens, antibodies, nucleic acids, enzymes, receptors, whole cells, and tissues (Damborský et al., 2016; Du and Dong, 2017). Owing to the cost-effectiveness and small size, in many areas, hands-on uses of optical biosensors are increasing, particularly in health care, biomedicine, and biopharma industry (Dey and Goswami, 2011; Yoo and Lee, 2016). Optical sensors can be categorized based on the type of transduction into absorption, resonance and photoluminescence (De Acha et al., 2017). The impressive models of different optical bio- and nano-aptasensors for identification of CTCs have been summarized in this part, based on the techniques used for transduction. Tables 1–3 presents a summary of the optical-based aptasensors for CTCs detection.

3.1. Luminescence-based CTCs aptasensors and nano-aptasensors

Photoluminescence consists of emission of light by a material as a consequence of its previous excitation. The quenching or enhancment of the intensity (or life-time) of this emission by the various target is a basis of luminescence-based biosensors (De Acha et al., 2017). In luminsense-based biosensor apparatus, various types of luminescent materials such as NPs, quantum dots (QDs), porphyrins, fluoropolymers and dyes (Roda et al., 2016) are usually entrapped or encapsulated into different matrices or shells, which must be designed to facilitate the interaction of the target with the sensing materials (Guan et al., 2015). Luminescence-based methods have been extensively investigated for biological assessments due to their great sensitivity, simple configuration, wide range of detection and low background noise (Iranifam, 2014; Roda et al., 2016). Accordingly, some CTCs aptasensors based on luminescence have been fabricated effectively (Table 1).

3.1.1. Enhanced chemiluminescence

In 2010, Bi et al., (2010a) applied a biobarcode dendrimer-like DNA (bbc-DL-DNA) as a tag for selective cancer cell detection alongside luminol–H_2O_2–Ru^{3+} chemiluminescence (CL) system. In this platform, a fourth era of macromolecule structures of bbc-DL-DNA (G_4 bbc-DL-DNA) was conjugated to complex aptamer-magnetic beads (MBs), through hybridizing linker DNA to the aptamer, followed by the RuNPs assembly on amine-functionalized beads. Upon addition of the target cell samples, the construction of a complex among target cells and aptamer, initiated the detachment of RuNPbbc-DL-DNA labels, which was oxidatively dissolved afterwards. Eventually, the CL system was used to assess the released Ru^{3+} cations. The CL intensity had a direct ratio to the concentration of the target cell receptor. The use of DL-DNA for signal intensification decreased the LOD of the method by 50 times, in comparison to the technique that used only one RuNP as a label. In addition to the simple magnetic isolation of immobilized aptamers, the suggested technique for analyzing cancer cells had higher sensitivity in comparison with other optical methods (Bi et al., 2010a; Chen et al., 2009; Nam et al., 2002).

In another project reported by Bi and co-workers, a multicomponent nanoprobe (CuS/DNA/Au/DNA/MNP) was used in a synergistic enhanced CL (SECL) approach for *in vitro* and *in vivo* determination of Ramos cells (B-cell human Burkitt's lymphoma). The detection level of this luminol-based SECL technique, obtained by a multi-element NP probe, was 56 cells mL^{-1} (Bi et al., 2010b). Another luminol-based CL assay with fixed aptamers on microfluidic channels was established to selectively identify and detach CTCs in blood samples. By capturing the CTCs with aptamer-functionalized AuNPs, the luminol–H_2O_2–AuNP measurable CL reaction was triggered. The calibration curve showed an acceptable linearity between the number of target cells and the CL intensity in 3 μL of the cell mixture with an LOD of 30 target cells. For validation, the spiked whole blood samples were also applied, using the real samples. Fabricated technique was inexpensive and requires less than 30 min to capture and detect target cells (Liu et al., 2011). In 2015, Wu et al. presented a paper-based microfluidic ECL origami cyto-device (μ-PECLOC), wherein aptamer-modified 3D macroporous Au-paper electrodes were used as the functional electrodes and well-organized scaffold for the precise identification of tumor cells. As a consequence of efficacious imbalance of H_2O_2 and unique identification of mannose on the exterior of the cell, NPs of AuPd alloy-conjugated concanavalin-A were included into this μ-PECLOC complex as the catalytically known nano labels for peroxydisulfate ECL system. A logarithmic relation was found between the ECL intensity and the concentration of MCF-7 cells, in the range of 450 to 1.0×10^7 cells mL^{-1} and LOD of 250 cells mL^{-1}. The suggested μ-PECLOC demonstrated outstanding analytical presentation with good repeatability, stability, and reliability, for sensing of tumor cells (Wu et al., 2015a).

A dual-potential ECL ratiometric mechanism was developed for CTCs detection and simultaneous assessment of cell surface glycan expression, in which two types of ECL nano-emitters, including luminol-reduced AuNPs and carbon nitride nanosheets (CNNS), as anodic and cathodic nano-emitters, respectively were implemented to achieve the dual-potential ECL. The CNNS were covered by means of AuNPs to bind to aptamer for the specific identification of CTCs, and the anodic nano-emitters were utilized with lectin to specifically detect surface glycans (Fig. 2). The proposed ratiometric ECL sensor revealed good analytical performance with a linear range of detection and an LOD of up to 20 cells, using MCF-7 CTCs as the sample target (Feng et al., 2016). Recently, Kun et al. introduced a "signal-on" switch ECL biosensor working based on nanocomposite and molecular recognition for identification of MEAR cells (a BALB/cJ mice liver cancer cell line) as CTCs in real samples. In the sensing platform, the glassy carbon electrode (GCE) surface was altered by the complex of Ru $(bpy)_3^{2+}$/β-cyclodextrin-AuNPs (β-CD-AuNPs)/graphene, pursued by the immobilization of ferrocene-labeled aptamers (TLS1c and TLS11a) as probes. The presence of CTCs as a target, led to the quencher (Fc) leave from the electrode surface, following conjugation of targets to aptamers thereby improving the ECL signal, i.e., recovering the "signal-on". This lately established ECL aptasensor revealed to be selective, supersensitive and rapidly detecting with an LOD of 40 CTCs mL^{-1}. The biosensor was also reusable with minimum 6 cycles to recover the initial signal (Kun et al., 2018).

Table 1
Comparison of the analytical performance of reported luminescence CTCs aptasensors.

Strategy	Cell	Sample	Aptamer sequence	Limit of detection (LOD)	Linear range (LR)	References
Luminol-based Enhanced Chemiluminescence	Ramos cells	Buffer	5′-GTGGCCCTCCTCTGGGACTTGTCGGTGGCTTGATAGGAGGGCCACAAGACAT-NH2-3′	62 cells ml^{-1}	100 - 1000 cells mL^{-1}	Bi et al. (2010a)
	Ramos cells		5′-NH2-TACAGAACACCGGGA GGATAGTTCGGTGGCTGTTCA GGGTCTCCTCCCGGTG-3′	56 cells ml^{-1}	80 - 100 cells mL^{-1}	Bi et al. (2010b)
	Ramos cells/CCRF-CEM cell line		5′-AACACCGGGAGGATAG TTCGGTGGCTGTTCAGGGTCTCCTCCCGGTG-3′	10 cells μL^{-1}	60 - 1500 cells 3 μL^{-1}	Liu et al. (2011)
	MCF-7 cells		5′-GCAGTTGATCCTTTG GATACCCTGGTTTTTTTTTTT–HS–3′	250 cells ml^{-1}	450–1.0 × 10^7 cells mL^{-1}	Wu et al. (2015a)
	HL-60 cells		5′- HS-TTTTTTTTTATCCAGAG TGACGCAGCATGCCCTAGTTACTACTACTCTTTTTAGCAAAC-3′			
	K562 cells		5′–HS–TTT TTT TTT TACAGC AGATCAGTCTATCTTCTCCTGATGGGTTCCTATTTATAGGTGAAG CTGT-3′			
	CCRF-CEM cells		5′-ATCTAACTGCTGCGCCGC CGGGAAAATACTGTACGGTTAGATTTTTTTTT–HS–3′			
	MCF-7 and HEK-293 cells		5′–HS–CACTACAGAGGTTGCGTC TGTCCCACGTTGTCATGGGGGGTTGGCCTG-3′	20 cells ml^{-1}	10^2-10^6 cells mL^{-1}	Feng et al. (2016)
	MEAR cells		TLS1c: 5′-ACAGGAGTGATGGTT GTTATCTGGCCTCAGAGGTTCTCGGGTGTGGTCA CTCCTG-3′-Fc TLS11a: 5′-ACAGCATCCCCATG TGAACAATCGCATTGTGATTGTTACGGTTTCCGCCTCATGGACGTGCTG-3′-Fc	40 cells mL^{-1}	200 - 1000 cells mL^{-1}	Kun et al. (2018)
Quantum dots (QDs)-based Luminescent	Ramos cells	Buffer	5′- SH-TACAGAACACCGGGA GGATAG TTCGGTGGCTGT TCAGGGT CTCCTC CCGGTG-3′	68 cells mL^{-1}	100 - 4000 cells mL^{-1}	Jie et al. (2011)
	CCRF-CEM cells	Buffer/ Blood	(SC2): 5′- ATCTAACTGCTGCGCCGCCGGGAAAATACTGTACGGTTAGA(A)6CTGCACGTCCGAC-3′ (SH2): 5′- CAGCCTGCACGTC(A)6ATCTAACTGCTGCGCCGCCGGGAAAATACTGTACGGTTAGA-3′	Not reported[a]	Not reported	Li et al. (2018b)
Rolling circle amplification	Ramos cells	Buffer	(SH2): 5′- CAGCCTGCACGTC(A)6ATCTAACTGCTGCGCCGCCGGGAAAATACTGTACGGTTAGA-3′	137 cells mL^{-1}	200 - 1000 cells mL^{-1}	Li et al. (2012)
	Ramos cells		biotin- TAGGCAGTGGTTTGACGTCCGCATGTTGGGAATAGCCACGCCT SH-AACACCGGGAGGATAGTTCGGTGGCTGTTCAGGGTCTCCTCCCGGTG	163 cells (3 σ)	0 - 2000 cells	Bi et al. (2013)
	Ramos cells		5′–SH–TAGGCAGTGGTTTGACGTCCGCATGTTGGGAATAGCCACGCCTATCTATCC	16 cells (3 σ)	20 - 500 cells	Chen et al. (2014b)
Upconversion luminescence	CCRF-CEM and K562 cells	Buffer	5′-thiolTTTTTTTTTTATCTAACTGCTGCGCGCCGGGAAAATACTGTACGGTTAGA	20 cells	Not reported	Fang et al. (2014)

[a] ~80% capture efficiency and purity.

Table 2
Comparison of the analytical performance of reported fluorescence CTCs aptasensors.

Strategy	Cell	Sample	Aptamer sequence	Limit of detection (LOD)	Linear range (LR)	References
GO-based aptasensors	SK-BR-3, PBMC, and HaCaT cells	Blood	S6: 5′GCGTGCGGAGCCAGGATGGGCGTGCGGAGCCAG A9: 5′GGGAGGACGAUGCGGACCGAAAAAGACCUGACUUCUAUACUAAGUCUACGUUCCCAGACGACUCGCCCGAGAAUUAAAUGCCCGCCAUGACCAG YJ-1: 5′GCGGAAGCGUGCUGGGCUAGAAUAAUAAUAAGAAAACCAGUACUUUCGU	~95% capture efficiency		Viraka Nellore et al. (2015)
Förster resonance energy transfer (FRET)	MDA-MB-231 cells	Buffer	5′GAAGTGAATATGACAGATCACAACT	300 cells ml^{-1}	1×10^3–4×10^4 cells mL^{-1}	Mohammadi et al. (2018)
Magnetic fluorescent-based aptasensors	MCF-7 cells	Buffer/ Blood	5′CAGCCTGCACTCTAACGCAGTTGATCCTTTGGATAGCCTGGGTTAGA	6 cells mL^{-1}	Not reported	Ding et al. (2018)
	BT474, and HELF cells	Blood	5′CACTACAGAGGTTGCGTCTGTCCCACGTTGTCATGGGGG	10 cells mL^{-1}	up to 50000 cells	Wang et al. (2018)
	HepG2, A549, and HEK293 cells	Buffer	5′-/5carboxyl/-CAC TACAGAGGTTGC GTCTGTCCCACGTTGTCATGGGGG GTTGGCCTG-3′	1.19 nM of EpCAM	2–64 nM of EpCAM	Cui et al. (2019)
Using of anti-EpCAM aptamer and flow cytometry imaging	Kato III, MDA-MB-231, T47D, HT-29, SW480, U11B-MG, Ramos, HEK-293T cells	Buffer	SYL3C: 5′-CACTAC AGAGGTTGCGTC TGTCCCACGTTG TCATGGGGGGTT GGCCTG-3′	~63% capture efficiency for positive cells with 80% purity		Song et al. (2013)
RNA aptamer conjugated to fluorochrome-quencher pairs	Karpas 299, SUDHL-1, HDLM2, KMH2, Mino, Maver-1, U937 cells	Blood	5′-GAUUCGUAUGGGUGGGAUCG GGAAGGGCUACGAACACCG-3′	Not reported		(Zeng et al., 2014)[a]
Silica NPs covered by highly branched dendrimer-amplified aptamer probes	Ramos cells and CCRF-CEM cells	Buffer	TD05: 5′-AACACC GGGAGGATAGTT CGGTGGCTGTTC AGGGTCTCCTCC CGGTGTTTTTTT TTT-3′-NH2 Sgc8 5′-ATCTAA CTGCTGCGCCGC CGGGAAAATACT GTACGGTTAGAT TTTTTTTTT-3′-NH2 Sgd5 5′-ATACCA GCTTATTCAATT ATCGTGGGTCAC AGCAGCGGTTGT GAGGAAGAAAGG CGGATAACAGAT AATAAGATAGTA AGTGCAATCT-3′-NH2	~90% capture efficiency		Zheng et al. (2014)
DNA aptamers labeled with Cy5 dye	Lung cancer specimens	Blood	LC-183: CTCCTCTGACTGTAACCACGATTTCGATCGCTCTGAGACT GCCAACGTCC CACCATTCGCGCATAGGTAG TCCAGAAGCC LC-17: CTCCTCTGAC TGTAACCACGCTTTTGTCTTTAGCCGAATTTTACTAAGCC GGGCTGATCAGCATAGGTAGTCCAGAAGCC LC-18: CTCCTCTGAC TGTAACCACGTGCCCGAACGCGAGTTGAGTTCCGAGAGCTCCGACTTCTTGCATAGGTAGTCCAGAAGCC LC-110: CTCCTCTGACTGTAACCACGTTAGGCGAGAACATGTCAGTACGTCGACGTTCTACTTGCTGCATAGGTAGTCCAGAAGCC	less then 2 cells per 3 ml of blood	1-22 cells per 3 ml of blood	Zamay et al. (2015)

[a] RNA aptamer.

Table 3
Comparison of the analytical performance of reported colorimetric, SERS, SPR and the other optical CTCs aptasensors.

Detection Method	Strategy	Cell	Sample	Aptamer sequence	Limit of detection (LOD)	Linear range (LR)	References
Colorimetric	Aptamer-conjugated gold NPs	Ramos cells and CCRF-CEM cells	Buffer	5′-TTTAAAATACCAGCTTATTCAATTAGTCACACTTAGAGTTCTAGCTGCTGCGCCGCCGGGAAAATACTGTACGGATAGATAGTAAGTGCA ATC T-3′ 5′-AACACCGGGAGGATAGTTCGGTGGCTGTTCAGGGTCTCCTCCCGGTG-3′	90 cells	1–5 × 10^4 cells	Medley et al. (2008)
	Self-assembly of a DNA concatemer to namerous sticky-ended three-way junctions	CCRF-CEM, Jurkat, Ramos, U937, and HepG2 cells	Buffer	5′-TTTATCTAACTGCTGCGCCGCCGGGAAAATACTGTACGGTTAGA	175 cells (3 σ)	175–1.5 × 10^4 cells	Norouzi et al. (2018)
	Aptamer-induced RCA on the cell surface	MCF-7 cells	Serum	$VEGF_{165}$ binding aptamer: 5′-GGGCCCGTCCGTATGGTGGGTGTGCTGGCTTTTAAAAAAAAAA -3′ MUC1 binding aptamer: 5′- GCAGTTGATCCTTTGGATACCCTGGTTTTTAAAA	10 cells mL^{-1}	10 - 30000 cells	Wang et al. (2015)
SERS	Aptamer conjugated MBs and SERS imaging	DLD-1 and CCRF-CEM cells	Buffer/ blood	Biotin-labeled and amino-labeled KDED2a-3 aptamer (5′-TGCCCGCGAAAACTGCTATTACGTGTGAGAGGAAAGATCACGCGGGTTCGTGGACACGGT TTTTTTTTTT-3′-biotin/amino)	as low as 20 cells mL^{-1}	20 - 1000 cells mL^{-1}	Sun et al. (2015)
	On-chip strategy combines size-based microfluidic cell isolation with SERS analysis	SKBR3,MCF7, MDA-MB-231, and Jurkat cells	Blood	EGFR: 5′ HS-C6-(T10)TACCAGTGCGATGCTCAGTGCCGTTTCTTCTCTTTCGCTTTTTTTTGCTTTTGAGCATGCTGACGCATTCGGTTGAC HER2: 5′ HS-C6-(T10) AACCGCCCAAATCCCTAAGAGTCTGCACTTGTCATTTTGTATATGTATTTGGTTTTTGGCTCTCACAGACACACTACACACGCACA EpCAM: 5′ HS-C6-(T10)TGAAGGTTCGTTGTTTCGGTGGGTGTAGACTCTTTAGAAGAGATACAGATTTTGGGAATG	-	10–20 cells for each cell type	Zhang et al. (2018)
SPR	Localized-SPR (LSPR) based on iSNMs	MDA-MB-231, MCF7, human fibrosarcoma, and HEK293T cells	Buffer	5′-AGCGTC GAATACCACTACAGAGGTTGCGTCTGTCCCACGTTGTCATGGGGGGTTGGCCTGCTAATGGAGCTCGTGGTCAG-NH2-3′	6.7 attoM for the EpCAM protein per one cell	-	Hong et al. (2016)
Other	SPM imaging coupled with a CNT-based patterned surface	LS174T cells	Buffer	5′GCGGAAGCGUGCUGGGCUAGAAUAAUAAUAAGAAAACCAGUACUUUCGU	<1 cell mL^{-1}	-	Kwon et al. (2013)
	Au NFs functionalized with MUC1-binding aptamer	Blood Samples Spiked with MCF-7 Cells	Buffer	AptMUC1: 5′-thiol-TTTTTT TTTTTTTTT GCAGTTGAT CCTTTGGAT ACCCTGG-3′	10 cells	0 - 1000 cells	Chiu et al. (2015)

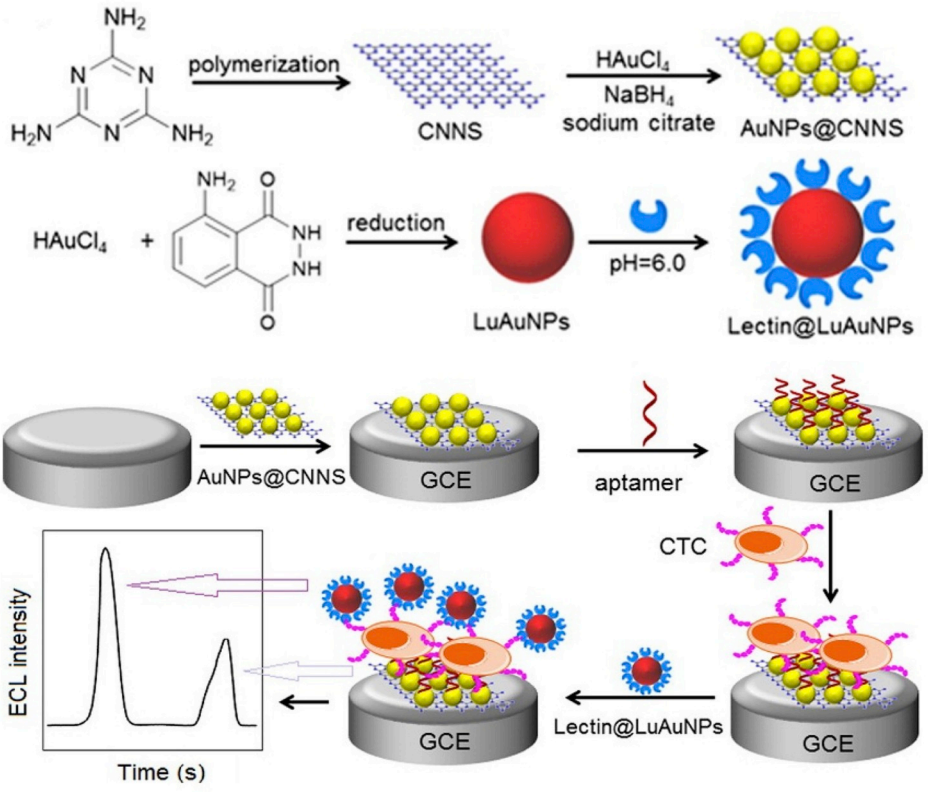

Fig. 2. Graphical representation of the construction of a ratiometric ECL strategy for detection of CTCs and evaluation of cell-surface glycan based on luminol-reduced AuNPs and carbon nitride nanosheets (CNNS). Reproduced with permission from (Feng et al., 2016).

3.1.2. Quantum dots (QDs)-based luminescent

Luminescent semiconductor QDs with specific characteristics, including size-dependent emission (Costa-Fernández et al., 2006), NP surfaces for versatile bio-conjugation, adaptable photo-physical characteristics for multiplexed capture, and higher stability for extended examination periods have a great potential for CTCs sensing. A dendrimer/CdSe–ZnS-QDs nanocluster (NC) was firstly used by Jie group as a probe for electro-chemiluminescence (ECL), to early and precisely

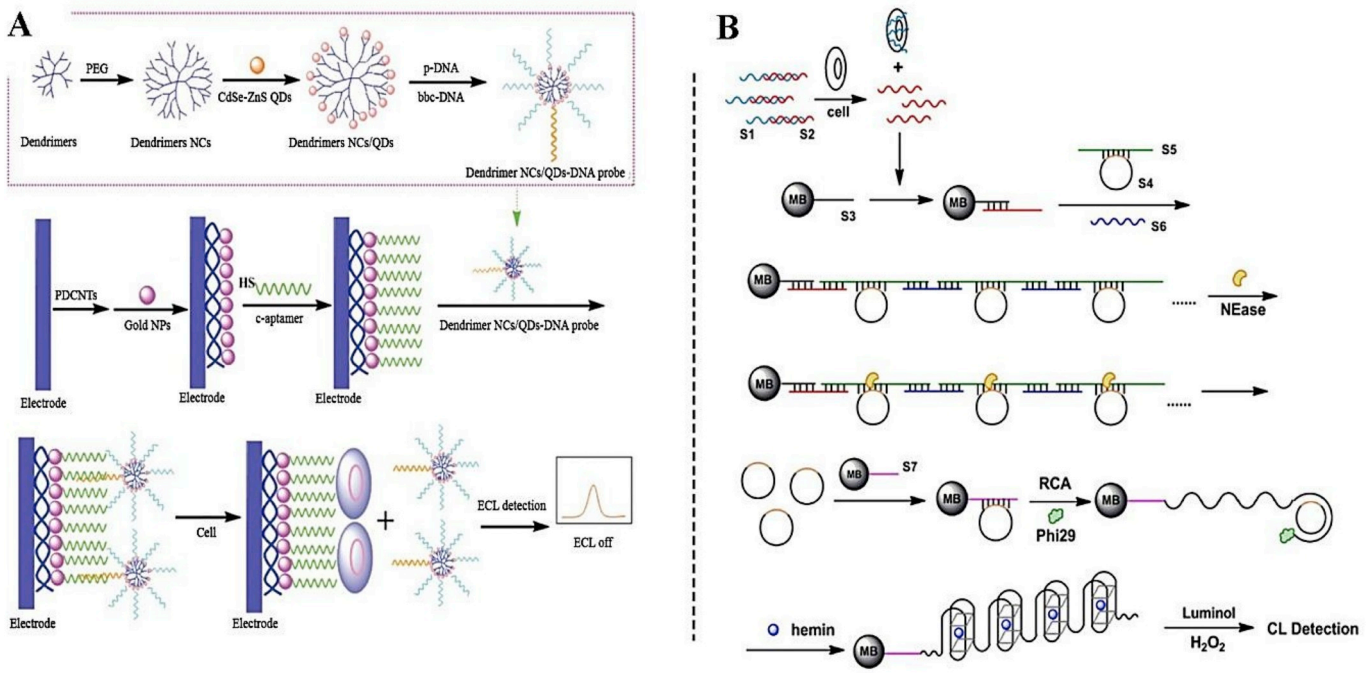

Fig. 3. (A) Fabrication steps of the dendrimer NCs/QDsDNA probe and ECL biosensor for signal-off detection of cells; (B) Schematic representation of cascade signal amplification strategy for the CL detection of the cancer cell. Reproduced with permission from (Jie et al., 2011) and (Li et al., 2012).

detect cancer cells. In this system, numerous CdSe–ZnS-QDs were decorated on the NC surfaces that could magnify the QD's ECL signal. Capture DNA was specifically created for the target cell as a high-affinity aptamer. In addition, MBs used to immobilize aptamers, were joined with the dendrimer/QD NCs probe for ECL signal testing of cancer cells. This combination with the aid of a cycle-amplifying technique, not only simplified the separation procedures, but also greatly improved sensitivity (Fig. 3a). The results showed an LOD of 68 cells mL^{-1} for cell concentration (Jie et al., 2011). Recently, MNP-QD-based aptasensor copolymers (MQAPs) was established for fast magnetic separation of CTCs. These MQAPs were fabricated by means of hybridization chain reaction to attain amplified magnetic response, remarkable binding affinity to target cells, providing ultra-bright cooperative QD PL for single cell detection. MQAPs are free of non-specific bindings, which would otherwise affect the pure capture of target cells. In this regard, the easy separation and counting of rare CTCs in blood samples with high sensitivity and precision could be achieved in 20 min (Li et al., 2018b). In using of QDs in CTCs aptasensors, it is important to note the toxicity, chemical instability, photo-bleaching and multi-exponential decay of QDs (Hötzer et al., 2012).

3.1.3. Rolling circle amplification

As a simple, well-organized and isothermal nucleic acid amplification mechanism, Rolling circle amplification (RCA) is becoming a

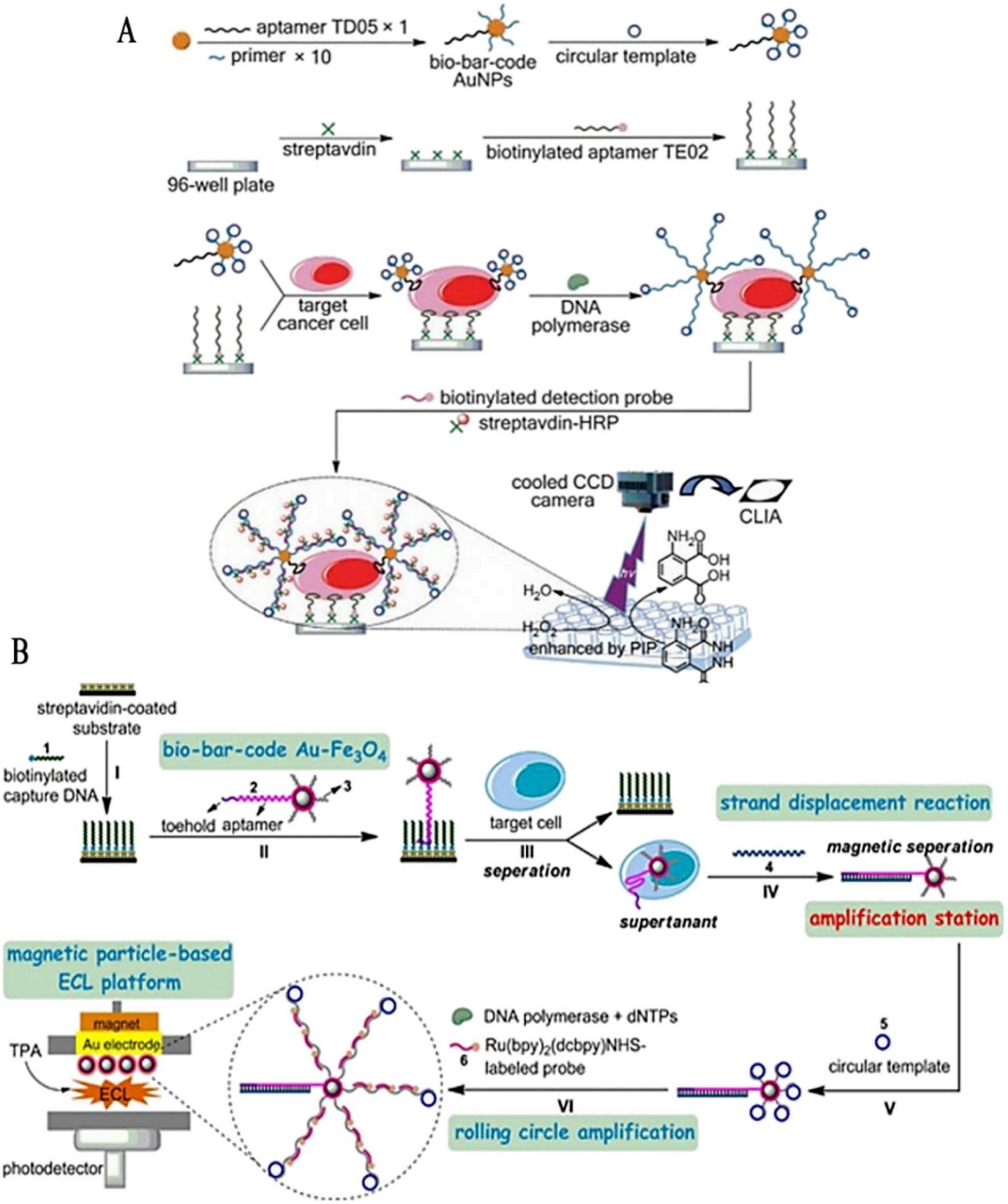

Fig. 4. (A) Schematic illustration of the proposed CLIA strategy for cancer cell detection through aptamer recognition and bio-bar-code nanoprobe-based RCA; (B) Illustration of the bio-bar-code magnetic particles based ECL platform for sensitive detection of Ramos cells by SDR and RCA. Reproduced with permission from (Bi et al., 2013) and (Chen et al., 2014b).

versatile method toward CTCs bioassays and biosensing method development (Ali et al., 2014; Li et al., 2012; Medley et al., 2008; Wang et al., 2019). Particularly, RCA integration with aptamers and NPs offers new opportunities for ultra-sensitive identification of biomolecules (Bi et al., 2013; Chen et al., 2014b; Lin et al., 2019), which can be further utilized as scaffolds for building nanostructures into one-dimensional superstructures (Gu et al., 2018). Accordingly, Li et al. established an RCA-based duplex probe, consisting of Ramos cells specific aptamers and complementary oligonucleotides. The Ramos cells implementation resulted in the separation of the complementary oligonucleotides, leading to circular DNA assembly and construction of the polycatenated DNA platform. When the circular DNA templates were recognized by a nicking endonuclease, they were dissociated into the DNA platform and initiated the RCA reaction to create a linear sequence of DNAzymes, subsequently accelerating the luminol-H_2O_2 CL (Fig. 3b). This proposed signal amplification process presented an LOD of 137 cells mL^{-1}. Nevertheless, the cancer-cell assessment is time-consuming and is performed at different temperatures (Li et al., 2012).

In another RCA-based CTCs detection study, a couple of aptamers with a capability of specific attachment to Ramos cells was applied. The first aptamer, TD05, was fixed as a reconnaissance probe on the AuNPs, and the second one, TE02, was attached to the 96-well microplate covered with streptavidin as a capture probe. By introducing the biobarcode AuNP probes, AuNP TD05 aptamers attached to the fixed Ramos cells to fabricate the AuNP-TD05-Ramos cell-TE02 complex (Fig. 4a). The RCA was then started on the AuNPs by introducing the Klenow DNA polymerase to generate a long ssDNA for building an enormous amount of biotinylated recognition probes, which then were tightly attached to streptavidin-conjugated horseradish peroxidase (HRP) to create the biobarcode AuNP probes with HRP label. Following elimination of the free streptavidin-HRP, the CL reaction was used to detect probes. Although the technique appears to be comparatively complex, the experimental procedure is fast, simple and inexpensive (Bi et al., 2013).

Furthermore, Chen et al. designed a different ECL-RCA-based aptasensor for the identification of CTCs. Briefly, biobarcode toehold-aptamer/DNA primer/Au–Fe_3O_4 (TA/DP/Au–Fe_3O_4) nanoconjugates were made-up and then fixed to the substrate *via* annealing aptamer to capture probe. The TA/DP/Au–Fe_3O_4 complex acts as the magnification spot to launch RCA, using strand displacement reaction (SDR). The result showed that a huge amount of Ru(bpy)$_2$(dcbpy) NHS-labeled probes were hybridized to RCA products, which were simply caught by the magnetic electrode to carry out the magnetic particle-based ECL scaffold (Fig. 4b). The suggested approach allows the Ramos cells identification as low as 16 cells, and shows great potential in clinical application (Chen et al., 2014b).

Despite numerous benefits, some challenges of the RCA system remain to be overcome for practical applications including making high-purity circular templates in high amounts and low efficiency of the enzymatic ligation step for creating small DNA circles (<30 nt). These issues can be addressed by using small amounts of DNA in the ligation mixture and chemical cyclization of DNA oligonucleotides capable of generating circular DNA molecules with a fairly acceptable outcome (up to 85%), respectively (Tang et al., 2012; Zhao et al., 2008). Moreover, nonspecific inter- and intra-molecular crosslinking may cause problems in use of RCA for cell targeting, which can be diminished by adjustment of an RCA product extent, rigidity, composition, and sequence. In the case of CTCs, it has been reported that incorporation of a polyT spacer between aptamer domains in the RCA product, can decrease the nonspecific communications between the aptamer and cancer cells (Tang et al., 2012). In conclusion, in order to minimize the aforementioned unwanted nonspecific interactions, computational methods, such as cadnano, can be employed to make predictable DNA nanostructures, using a good design RCA sequence and staple strands.

3.1.4. Upconversion nanoparticles

Recently, upconversion nanoparticles (UCNPs) have demonstrated numerous benefits as fluorescence probes, owing to their high chemical and photochemical stability, high signal-to-noise ratio, low toxicity, large stokes shifts, and resistance to photo-bleaching (Chen et al., 2014a; Yang, 2014). UCNPs are a type of luminescent NPs which can convert near-infrared (NIR) excitation light into visible and ultraviolet emission light. The critical aspect of UCNPs is that they have a low signal to noise ratio, high penetration depth into biological sample and diminish the autofluorescence background (Wilhelm, 2017). These unique optical properties make them ideal for many applications, including sensing, imaging, diagnosis and therapy (Wen et al., 2018).

In this aspect, the UCNPs were used for biological detection, imaging and even treatment of cancer (Cheng et al., 2010; Idris et al., 2012; Wang et al., 2011). For the CTCs detection purposes, Fang et al. used aptamer-conjugated UCNPs as nanoprobes to identify tumor cells. In this strategy, firstly CTCs were recognized *via* the UCNPs-aptamer-biotin complex, which is then identified by avidin-conjugated magnetic nanoparticles (MNPs) (Fig. 5). After magnetic isolation, upconversion luminescence (UCL) imaging was carried out to identify the CTCs. In this approach, without significant damage (viability~83%), the purities of identifying cells were reported up to 89% in blood samples containing 1000 tumor cells. The results also showed a reduced background signal and a reasonably good linear correlation between the number of captured cells and UCL intensity (Fang et al., 2014).

Despite the attractive properties of UCNPs for biosensing applications, a number of limitations such as synthesis and surface modification of UCNPs, enhancement of the brightness and emission efficiency of UCNPs and the revision of quality of UCNPs still need to be addressed for the commercial applications of UCNPs (Wilhelm, 2017).

3.2. Fluorescence-based CTCs aptasensors and nano-aptasensors

As a highly sensitive, reproducible, rapid, and non-destructiveness process, fluorescence analysis has been widely used in both bioanalytical chemistry and developing biosensor technologies. Fluorescence detection often consist of a source of excitation light, a fluorophore, wavelength filters to separate photon emissions from excitable molecules, and a detector that picks up the intensity of the fluorescence (Pires et al., 2014). There are several conventional fluorescent or quencher molecules, which provide very sensitive detection. These different dye molecules can be easily paired with nucleic acid

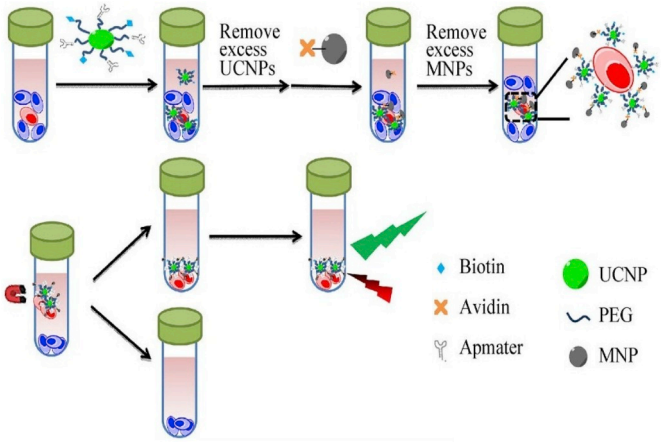

Fig. 5. Schematic representation of CTCs detection, using UCNPs-aptamer-biotin and MNP-avidin nanoprobes. Positive tumor cells are specifically recognized by UCNPs-aptamer-biotin nanoprobes, which are then attached by MNPs-avidin NPs for magnetic separation. The UCL signals from UCNPs could be used for tumor cell detection. Reproduced with permission from (Fang et al., 2014).

aptamers and can be identified in actual time detection (Dickey and Giangrande, 2016). In this regard, numerous fluorescent aptasensors have been developed for detection of CTCs based on various mechanisms, including graphene oxide (GO), Förster resonance energy transfer (FRET), and Magnetic fluorescent, etc.

3.2.1. Graphene oxide-based aptasensors

Recently, GO as a fluorophore has been receiving an extreme amount of attraction in aptasensors design, because of their great quenching property, well stability, excellent conductivity, tunable optical properties for optical read-outs such as fluorescence and plasmonics and simple surface alteration ability for bio-conjugation (Loh et al., 2010; Szunerits and Boukherroub, 2018; Wang et al., 2010), which make it favorable sensing composite (Dong et al., 2010). In 2015, Viraka Nellore et al. developed an aptamer-modified porous GO membrane for identification of different types of CTCs with multicolor fluorescence imaging. In their study, three distinct kinds of aptamers were covalently bound to a 2D GO membrane through amide bonds between carboxyl groups of GO and amine groups of functionalized aptamers. Results showed that dye-altered aptamers S6, A9 and YJ-1 bound to porous GO membranes are able to selectively capture numerous kinds of tumor cells (SW-948 colon cancer cells, LNCaP prostate cancer, and SKBR3 breast cancer) with efficiency about 95%. Aptamer-attached membranes mentioned here, are capable of early detection of CTCs that are presently being identified by cell-capture based sciences (Viraka Nellore et al., 2015).

Various factors including the intrinsic fluorescence of some serum proteins, the background noise, temperature and pH can alter the sensitivity of the GO-based platforms for CTCs detection (Ping et al., 2015). Thus utilizing fluorophores with time-resolved fluorescence characteristics (Hötzer et al., 2012), the optimization of spectra, and chemical-surface modification should be noted (Costa-Fernández et al., 2006). GO-based aptasensors for CTCs detection are still in their infancy. For commercialization of these aptasensors, the non-specific interactions, the large-scale reproducibility and toxicity and biocompatibility issues still need to be addressed (Szunerits and Boukherroub, 2018).

3.2.2. FRET-based aptasensors

FRET method is another interesting sensing technology, which has been increasingly utilized to develop quick, selective and practical bioanalytical assays. In FRET process, overlap between donor photoluminescence and acceptor absorption cause relaxation of the donor to a nonfluorescent ground state, which excites fluorescence in the acceptor (Zhang et al., 2019a). In many FRET-based tests, the specific photophysical and optical characteristics of fluorescent NPs have been stated to be effective acceptors and/or donors for the substitution of fluorescent organic dye molecules (Das et al., 2018).

In this regard, Mohammadi et al. proposed a FRET-based aptasensor with an extremely biospecific association between carcinoma antigen 15-3 (CA 15-3) and the associated antibody. In the proposed method, AuNPs labeled PAMAM-dendrimer/aptamer and anti-CA 15-3 antibody-conjugated carbon dots were utilized as acceptor/donor, respectively. As CA 15-3 antigen was introduced into the reaction, the robust interaction between CA 15-3-aptamer and anti-CA 15-3 antibody held carbon dot and AuNPs complex pair closer thereby reducing the fluorescence signal. The LOD of the FRET immunoassay measured to be 0.9 μU mL^{-1}. This method showed acceptable specificity and sensitivity for MDA-MB-231 breast cancer cell counts from 1000 to 40000 cells mL^{-1}, with an LOD of 300 cells mL^{-1} (Mohammadi et al., 2018).

The cost of FRET reagents, enhancment of fluorescent resolution, improvement of specificity of the reaction and increasing the signal-to-noise ratio and real-time dynamic monitoring of physiological conditions are probable main barrier for the development of FERT-based aptasensors for CTCs detection (Zhang et al., 2019a).

3.2.3. Magnetic fluorescent-based aptasensors

Inclusion of scaffold materials such as magnetic beads in the fabrication of aptasensors can improve the performance of aptasensor (Zhou et al., 2020). Magnetic poropertise of MNPs can help to manage the sensing systems by improving the separations and loading processes in aptasensing device (Hayat et al., 2013). Moreover, it is simple to functionalize the surface of MNPs with divers type of chemical functional groups (e.g. polymers, silica and noble metals) (Modh et al., 2018).

Recently, MNPs are employed for the specific capture and detection of CTCs. For example, a "turn-on" magnetic fluorescent biosensor was developed by Cui et al. which was consisted of Fe_3O_4, molybdenum disulfide (MoS_2) nanosheets, and graphene quantum dots (GQDs). In this system, aptamer/Fe_3O_4/GQD complex and MoS_2 nanosheets, as a fluorescence quencher, were assembled to build "turn-on" biosensing magnetic-fluorescent nanocomposites (MFNs) (Fig. 6). With an average capture effectiveness of 90%, an LOD of 10 CTCs mL^{-1}, and quick identification and labeling CTCs within 15 min, MFNs have the potential to be used for fluorescence-guided tumor cell enrichment and bioimaging (Cui et al., 2019). A novel near-infrared probe depending on Ag_2S nanoassembly has been created for sensitive detection and extremely effective capture of CTCs in bloodstream, by mixing it with anti-EpCAM (epithelial cell adhesion molecule)-MNs. The method was successfully used for the fabrication of near-infrared fluorescent Ag_2S nanoprobe *via* hybridization chain reactions by means of aptamer-modified Ag_2S nanodots, which can greatly reduce the background signals and increase the imaging sensitivity. Moreover, the anti-EpCAM antibody-labeled magnetic nanospheres were applied for extremely unusual CTCs capture in whole blood samples. The near-infrared nanoprobe with signal amplification and immune-magnetic spheres (IMNs) scaffold showed an outstanding presentation for effective capture and detection of CTCs, with an LOD of 6 cells mL^{-1} in mimicking whole blood (Ding et al., 2018).

Another remarkable system consisted of an anti-EpCAM aptamer assembled pseudo-DNA nanocatenane (PDN) and HER2-coated MBs was utilized for double targeting and isolating CTCs. In this system, signal amplification for CTCs detection was based on the conjunction of RCA and MBs. The HER2-coated MBs isolated CTCs from blood, following their elution from a magnetic column. The specific PDN, which is tailor-made self-assembly of three circular DNAs, bound to CTCs through EpCAM. The system collectively created improved fluorescent signals for extremely sensitive recognition of CTCs in the existence of MB, phi29 DNA polymerase and RCA primers. By means of this system, an LOD of 10 CTCs mL^{-1} was achieved. This system is practical, highly-sensitive, and adequately suitable for the identify of breast CTCs in the laboratory (Wang et al., 2018).

3.2.4. Other mechanisms

Additionally, other mechanisms introduced some novel bioengineering techniques, which have been applied to develop fluorescent aptasensors for CTCs detection. The information and their details have been listed in Table 2. (Song et al., 2013; Zamay et al., 2015; Zeng et al., 2014; Zheng et al., 2014). Table 2 presents a summary of the fluorescence-based aptasensors for CTCs detection.

3.3. Colorimetric-based CTCs aptasensors and nano-aptasensors

Several sensitive, non-apparatus detection methods have been described to convert the binding events of the aptamer-target into relative detectable color changes (Song et al., 2012; Wang et al., 2015). Due to robustness under various conditions and cost-effectiveness, colorimetric assays are one of the most frequently used methods in cancer cells detection (Du and Dong, 2017). The colorimetric-based assays are easy to use, which simply depend on the existence of the target molecules with no requirement for an expensive quantification apparatus (Hutter and Maysinger, 2013). In 2008, a research team proposed a method in which aptamer-conjugated AuNPs were used to

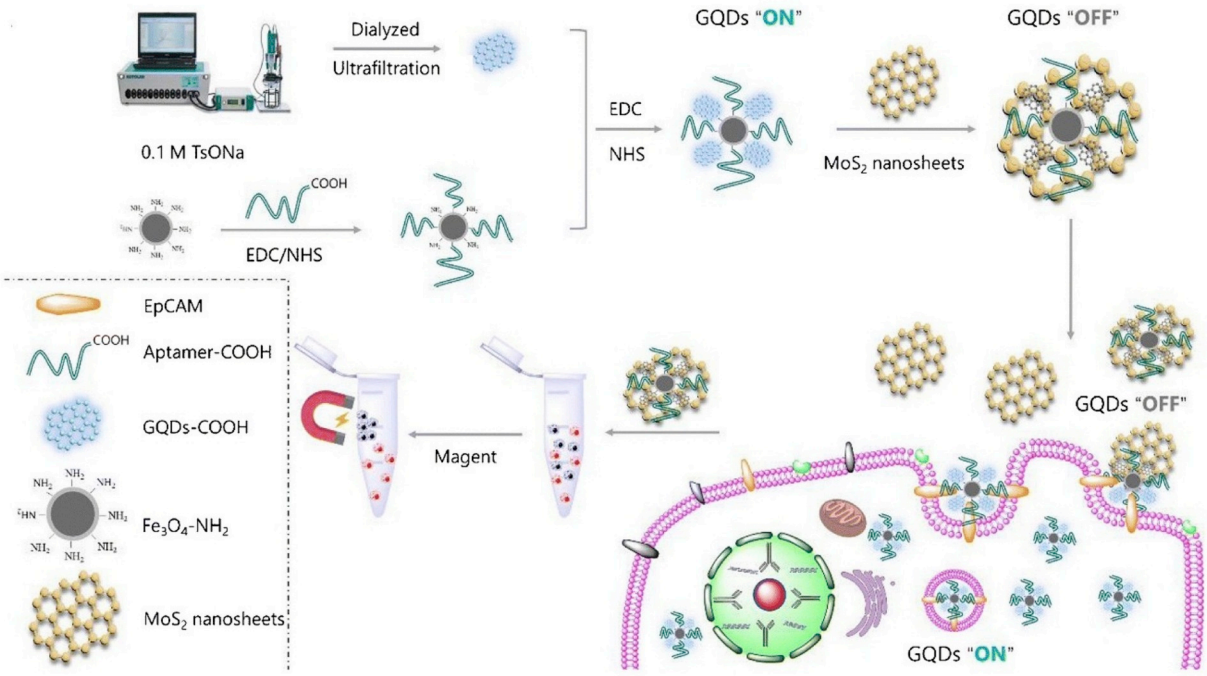

Fig. 6. The sensing mechanism of the aptamer/Fe_3O_4/graphene quantum dot (GQD)/MoS_2-based nanosurface energy transfer biosensor for the detection of CTCs. EDC: 1-ethyl-3-(3-dimethylaminopropyl) carbodiimide, NHS: N-hydroxysuccinimide, TsONa: sodium toluenesulfonate. Reprinted with permission from (Cui et al., 2019).

integrate the affinity and selectivity of aptamer, and the spectroscopic benefits of AuNPs to develop a sensitive detection of cancer cells. Non-target samples did not produce any change in color, but samples containing target cells showed a significant color change. The LOD of the target cells was calculated to be 90 cells (Table 3) (Medley et al., 2008).

Some research groups offer colorimetric assays based on G-quadruplex DNAzymes with peroxidase activity as signal-amplifying components for ultrasensitive detection of CTCs (Table 3). Norouzi et al. developed a functional nano-assembly of DNA that can identify cancer cells (Norouzi et al., 2018). DNA nano-assemblies were built by the self-association of a DNA concatemer to numerous sticky-ended three-way junctions. While the nano-assembly was directed to the target cell by an aptamer moiety, the peroxidase inserted in the nano-assemblies was employed to produce colorimetric signals as a sensing element. The result showed that the LOD was about 175 cells, which was almost ~5 folds smaller than the split DNAzyme technique with no amplification (Shi et al., 2014a). To ameliorate the sensitivity of G-quadruplex DNAzyme based colorimetric sensors, numerous systems such as RCA

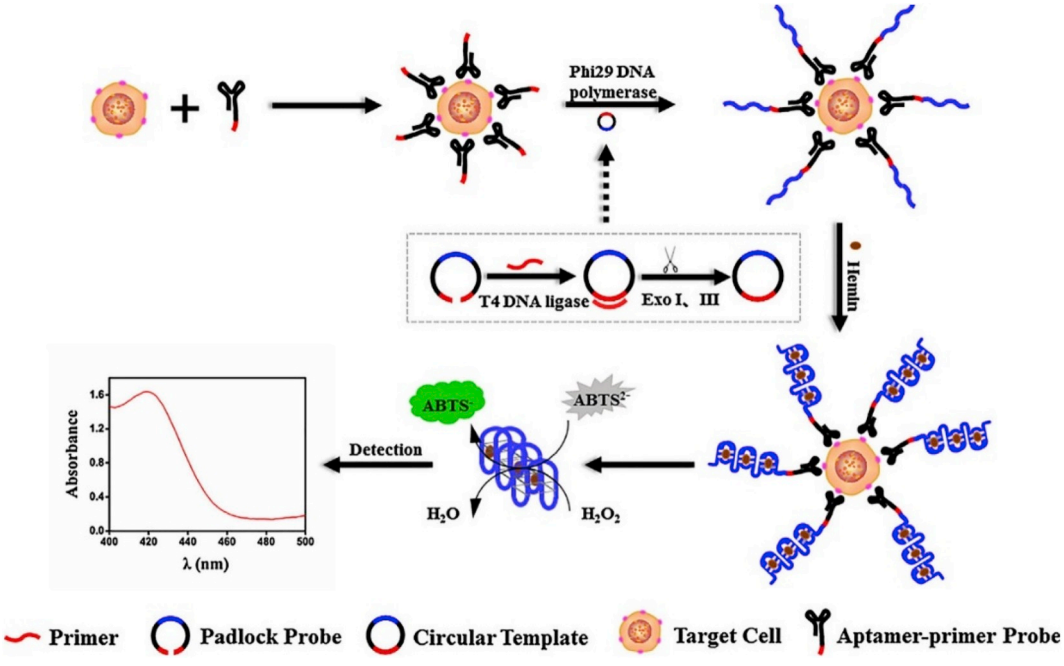

Fig. 7. Schematic representation of the colorimetric assay of tumor cells by aptamer-induced RCA on the cell surface. Reprinted with permission of (Xu et al., 2018).

(Jiang et al., 2014), PCR (Bhadra et al., 2014), autonomous DNA machine (Zheng et al., 2014) and strand displacement amplification (Du et al., 2016) have been employed. In this line, a pragmatic colorimetric strategy was conducted by Xu et al. for the detection of CTCs based on aptamer-induced RCA on the surface of the cell. In this method, an EpCAM-targeted aptamer was chosen as a recognition element and used for *in situ* aptamer-induced RCA with great G-quadruplex sequences on the exterior of the cell (Fig. 7). The G-quadruplex/hemin DNAzyme complex was then created which accelerated a colorimetric response for CTCs detection. The designed colorimetric assay with an LOD of 10 cancer cells in 10000 times of benign cells, showed very high selectivity and sensitivity (Xu et al., 2018). Table 3 presents a summary of the colorimetric-based aptasensors for CTCs detection.

Besides the many benefits of colorimetric aptasensors, there are some disadvantages e.g. pH/temperature impressible, tedious measurement circumstances, difficult sample handling and preparation as well as sensitivity to changes in the experimental geometry (Mehmood et al., 2019).

3.4. SERS-based CTCs aptasensors and nano-aptasensors

Surface-enhanced Raman spectroscopy (SERS) is an advanced vibrational spectroscopy that has turned into a common detection and optical imaging device, owing to its powerful signal intensity, biocompatibility, outstanding photostability, and particularly the multiplexing capability (Cialla et al., 2014). In this kind of spectroscopy, the excitation of localized surface plasmon resonances (LSPR) at the surface of nanostructured metals with light leads to induction of the massive intensification of the Raman scattering from the molecules located near the metal surface. This effect results in an ultrasensitive plasmon-enhanced spectroscopic method that enhances the inherent structural specificity and experimental flexibility of Raman spectroscopy (Guerrini and Alvarez-Puebla, 2019). SERS is one of the highly sensitive methods to detect and identify CTCs (Nima et al., 2014; Ranc et al., 2013; Sha et al., 2008; Shi et al., 2014b; Sun et al., 2015; Wang et al., 2013; Zhang et al., 2014). The earliest record of CTCs detection using SERS with specific aptamers was succeeded by Sun et al. with the help of aptamer-conjugated MBs, in which SERS image was obtained and CTCs were enriched and separated. The capture efficiency was 55% and 73% in the blood sample and buffer, respectively. In comparison with conventional approaches, this aptamer-based SERS method can find the source of tumor metastasis and the particular tumor (Sun et al., 2015). A recently proposed on-chip strategy combines SERS analysis with size-based microfluidic cell isolation for *in situ* profiling of CTCs. In this study, the gap size of the microfluidic filter was corrected to achieve a great purity and capture rates of CTCs (Fig. 8a). Based on their composite spectral signatures, the phenotypic data of captured CTCs was easily achieved by the revised classic least square algorithm, using spectrally orthogonal SER probes. In this system, cells from various subtypes of breast cancer can be categorized with high specificity and sensitivity (Zhang et al., 2018).

There are still some obvious flaws about SERS-based detection techniques for CTCs, which lead to unsatisfactory results in detection or characterization of the target (Zhang et al., 2017). Firstly, these techniques require an initial enrichment step for capturing CTCs in whole blood, which makes the process of detection more complicated. The process of enrichment is completely dependent on the unique communication between specific receptors expressed on the surface of cancer cells and recognition agents, mostly antibodies. Since antibodies are usually expensive, the high expenses of the technique significantly limits the use of SERS-based detection of CTCs in routine clinical diagnosis. Secondly, accurate and multidimensional characterization of the analyte cannot be achieved by vibration information from the SERS spectrum alone (Ukaegbu et al., 2016). Recently, there has been extensive research regarding the development of SERS in combination with various technologies for high-performance CTCs detection and characterization (Li et al., 2015; Wu et al., 2015b; Yao et al., 2013).

3.5. SPR-based CTCs aptasensors and nano-aptasensors

One of the most powerful tools for the study of kinetic properties of biomolecular interactions is surface plasmon resonance (SPR)-based

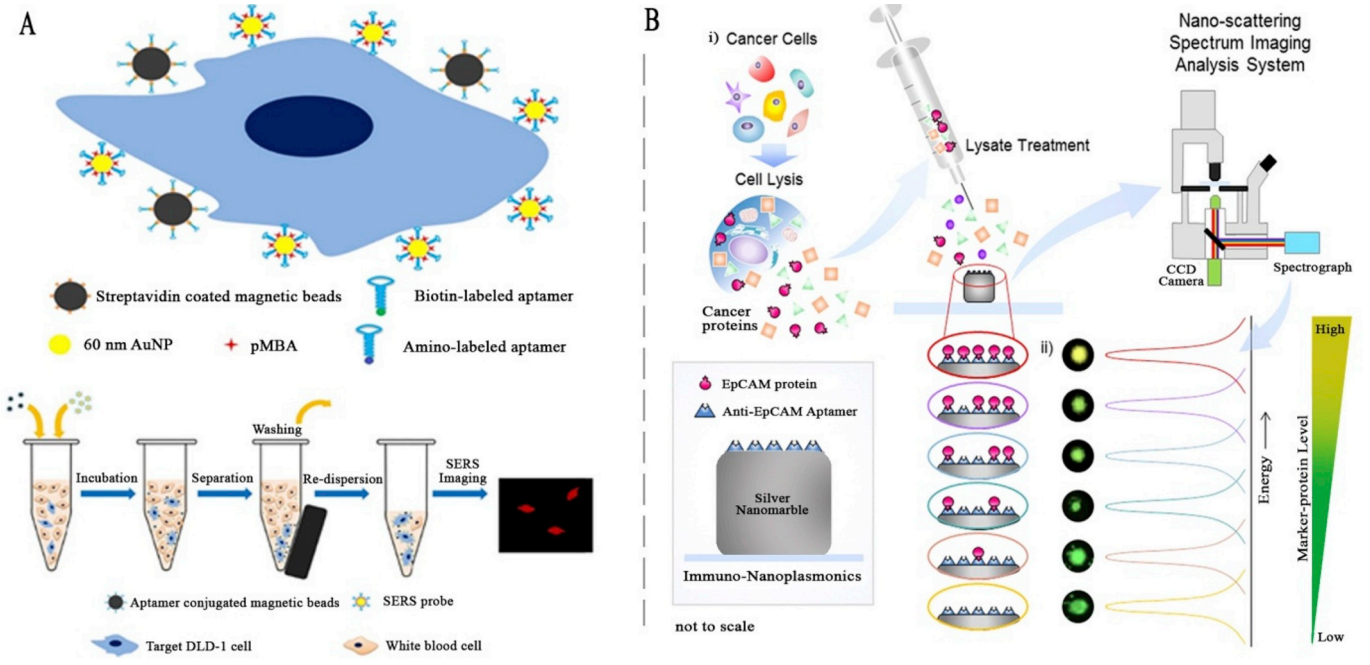

Fig. 8. (A) Schematic description of CTCs capture and identification, using Apt-MBs and SERS imaging; (B) Schematics for precise analysis of cancer biomarker based on anti-EpCAM aptamer-conjugated silver nanomarble (iSNMs) and the nano-scattering spectrum imaging analysis (NSSIA) system. (i) The extracted EpCAM proteins from target cancer cells are treated with iSNMs for LSPR-based protein sensing. (ii) Energy grading of representing specific color from the LSPR signal, using NSSIA to analyze biomarker expressions. Reprinted with permission from (Sun et al., 2015) and (Hong et al., 2016).

biosensors (Anker et al., 2008; Kabashin et al., 2009; Šípová and Homola, 2013). SPR biosensors use a certain mode of the metal-dielectric waveguide (a surface plasmon) to evaluate changes in the refractive index induced by the biomolecular interaction taking place at the surface of the SPR biosensor (Wijaya et al., 2011).

NPs are able to improve the sensitivity of SPR-based biosensors, as used on nearby to the SPR substrate leading to considerable change in the SPR-related peak position. Presently, SPR-based biosensors have achieved significant progress in many areas, particularly in cancer marker detection. In this regard, Hong et al. described an *in vitro* biomarker sensor, using localized SPR (LSPR) based on immunosilver nanomarblies (iSNMs) and a nano-scattering spectrum imaging analysis (NSSIA) system. Especially, highly monodisperse SNMs with high-quality images were prepared and the sensing substrates were also constructed using the NP adsorption technique. For precise sensitive and selective identify of EpCAMs expressed on CTCs, the exterior of the SNM was covered with an anti-EpCAM aptamer (Fig. 8b). Collectively, they have established a biomarker-detectable LSPR sensor dependent on iSNMs, with an LOD of 67 fM for the EpCAM protein (Hong et al., 2016).

SPR-based detection methods of CTCs do not need a label to detect the event, thus avoiding a separation step to remove the label (Costa et al., 2014). However, elevation of background refractive index mainly due to cross-reactivity can be challenging in both real and complex samples (Nguyen et al., 2015). This concern can be overcome by optimizing the accurate binding of the CTCs aptamers to a specific target. Furthermore, existing SPR instruments remain large and expensive, and this is still a barrier for marketing SPR technology. To achieve this goal, additional studies on the establishment of innovative chip chemistry, combined with miniaturization and amplification schemes, will be required to prepare SPR as a routine point-of-care (POC) diagnostic tool (Nguyen et al., 2015).

3.6. Other optical-based CTCs aptasensors and nano-aptasensors

Currently there are other reported optical-based aptasensors have been fabricated based on various strategies (Table 3), for example Kwon

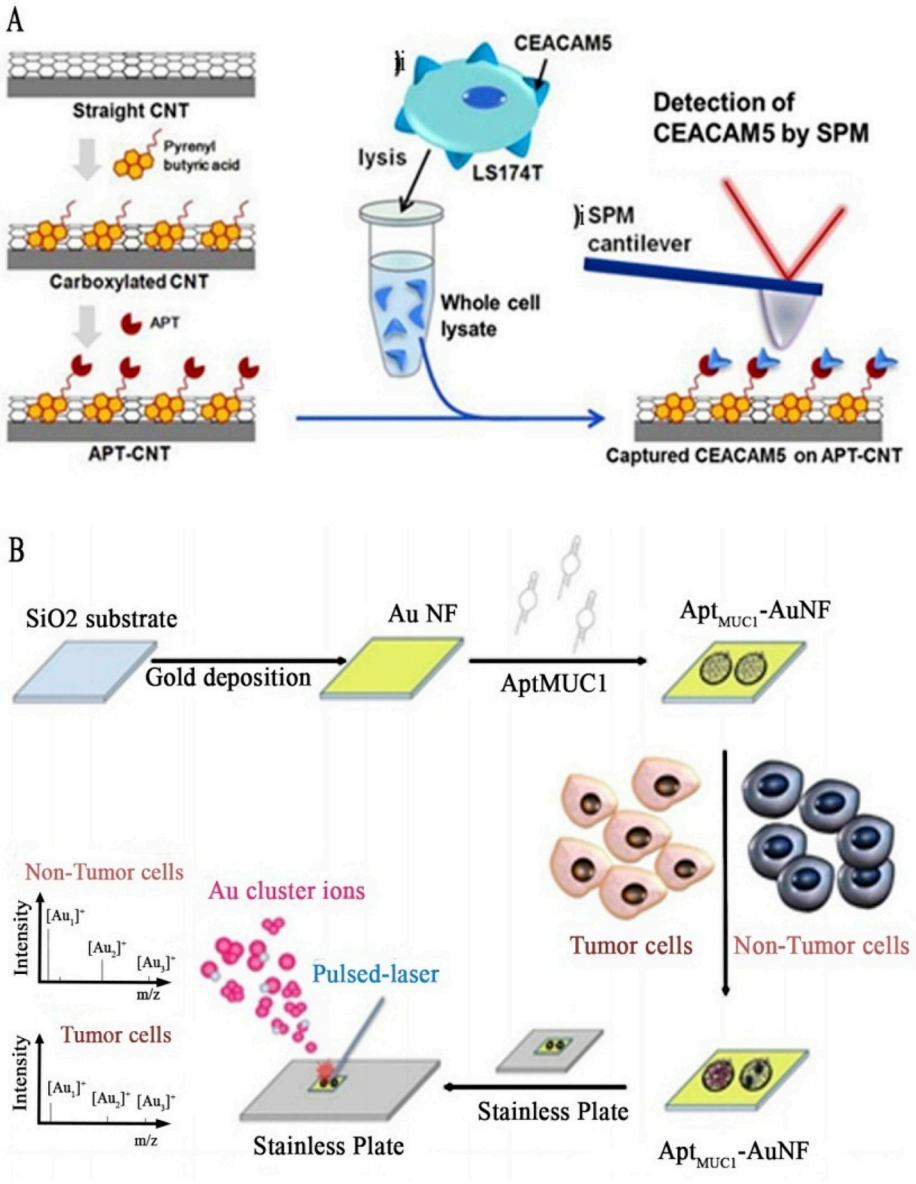

Fig. 9. (A) The fabrication of a patterned surface based on a CNT functionalized with an aptamer. (i) SPM-based detection of CEACAM5 captured by ACNT. (ii) CEACAM5 molecules expressed on CTCs were obtained from the whole lysate of colon cancer LS174T cells; (B) AuNFs for the enrichment of targeted and detection of tumor cells coupled with LDI-MS. Reprinted with permission from (Kwon et al., 2013) and (Chiu et al., 2015).

Table 4
Electrochemical aptasensors and nano-aptasensors for detection of CTCs.

Strategy	Cell	Sample	Aptamer sequence	Limit of detection (LOD)	Linear range (LR)	References
PDMS chip consisted of a cover and microelectrode matrix on a silicon dioxide layer	Rat-derived primary meningeal fibroblasts	Buffer	(5′-GGCGCUCCGACCUUAGUCUCUGUGCCGC UAUAUGCACGGAUUUAAUCGCCGUAGA AAAGCAUGUCAAAGCCGGAACCGUGUA GCACAGCAGAGAAUUAAAUGCCCGCCA UGACCAG-3′)	1 cell	1-26 cells	(Wang et al., 2012)[a]
Conjugating dual aptamers to the surface of a GCE	MEAR cells	Blood	K88: 5′-T15GGCGACCCCCGGGCTACCA GACAATGTACGC-3′) TBA: 5′-T15GGTTGGTGTGGTTGG-3′ TLS1c: 5′-T15ACAGGAGTGATGGTTGTT ATCTGGCCTCAGAGGTTCTCGGGTGTGG TCACTCCTG-3′ TLS11a: 5′-T15ACAGCATCCCCATGTGA ACAATCGCATTGTGATTGTTACGGTT TCCGCCTCATGGACGTGCTG-3′	1 cell	1-14 cells	Qu et al. (2014)
Formation of aptamer-protein-bead sandwich on the surface of electrode	Crude blood plasma samples from lung cancer patients	Serum	LC-18: 5′-CTCCTCTGACTGTAACCAC GTGCCCGAACGCGAGTTGAGTTCCG AGAGCTCCGACTTCTTGCATAGGTA GTCCAGAAGCC	0.023 ng mL^{-1}	230–0.023 ng mL^{-1}	Zamay et al. (2016)
A label-free electrochemical impedance spectroscopy aptasensor	MCF7 and HeLa cells	Buffer	5′-AACAGAGGGACAAACGGGGGAA GATTTGACGTCGACGACATCCGCU GAUUUGAAUCCUAACG-3′	10 cells mL^{-1}	30–1 × 10^6 cells mL^{-1}	Shen et al. (2016)
Array nanochannel-ionchannel hybrid combined with electrochemical detection technique	CCRF-CEM, k562, and Ramos cells	Buffer	sgc8c: 5′-ATCTAACTG CTGCGCCG CCGGGAA AATACTGTACGGTTA G ATTTTTTTTTT-3′-(CH2)6–NH2	100 cells mL^{-1}	100 - 1000 cells mL^{-1}	Cao et al. (2017)
Aptamer probe and *in situ* layer-by-layer assembly of dendritic structure (DS) nanoprobes	HepG2 cells	Blood	TLS11a: 5′-ACAGCATCCCCATG TGA ACAATCGCATTGTGATTGTTACGGT TTCCGCCTCATGGACGTGCTG-3′	5 cells mL^{-1}	37.6–5.6 cells mL^{-1}	Sun et al. (2018)
Immune-MBs are used for both separation and enrichment of CTCs and as enzyme mimics with rGO/MoS_2 synergistic catalysis for signal amplification	MCF-7, MDA-MB-231, SK-BR-3, A549, and H460 cells	Buffer	TLS11a: 5′-T15ACAGCATCCCCATGTGAACA ATCGCATTGTGATTGTTACGGTTTCCGCCTCA TGGACGTGCTG-3′	6 cells mL^{-1}	15 - 45 cells mL^{-1}	Tian et al. (2018)
Signal enhancement system based on tyramide signal amplification	HeLa cells	Buffer	AS1411: 5′-TTGGTGGTGGTGGTTGTGGTGGTGG TGG-3′ NH2	2 cells mL^{-1}	2–2 × 10^4 cells mL^{-1}	Zhou et al. (2019)
Integrated microfluidic chip equipped with FETs sensor arrays	HCT-8 cells	Blood	5′-TACAGCACCACAGACCATGGTTGTGTTTTTTTTTG TGTGGCTTCGTATGTTGTTGCGTGTTTGTCTTCCTGCC-3′	42 cells	Not reported	Chen et al. (2019)

[a] RNA aptamer.

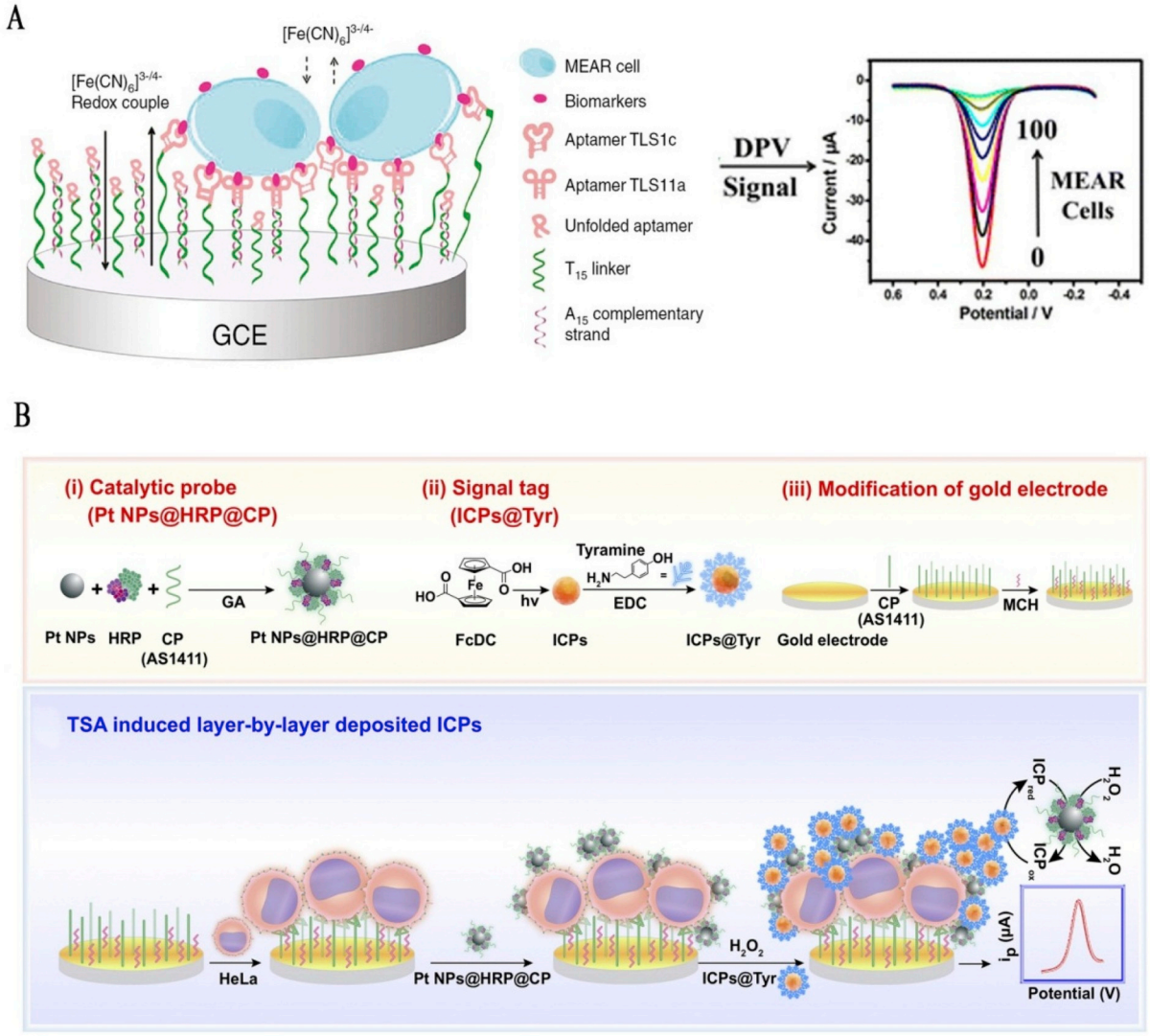

Fig. 10. (A) Scheme of the dual-aptamer modified electrode interface for specific and sensitive detection of MEAR tumor cells and a representative DPV measurement; **(B)** The principle of electrochemical immunosensor for CTCs detection based on TSA induced layer-by-layer deposited ICPs. Reprinted with permission from (Qu et al., 2014) and (Zhou et al., 2019).

et al., presented a highly sensitive and label-free detection methods for carcinoembryonic antigens (CEAs), expressed on CTCs using scanning probe microscopy (SPM) imaging, paired with a carbon nanotube (CNT)-based patterned surface. In this approach, for the construction of a CNT-patterned surface, straight CNTs were chemically formed on a silicon substrate, and modified with pyrenyl molecules, leading to the chemical activation of CNTs with aptamers for the unique detection of CEAs. For the sake of label-free identification of CEAs by means of a CNT-patterned surface, the SPM imaging method was used to display CEAs particularly linked to a CNT-based patterned surface (Fig. 9a). Their sensing method detected not only a single isolated CTC, but also CEAs expressed on a few CTCs with a concentration of less than 1 cell mL^{-1}. Specifically, their sensing technique enabled the identification of CEA proteins even at the isolated molecule determination (Kwon et al., 2013).

Chiu et al. demonstrated the utilization of the pulsed laser desorption/ionization mass spectrometry (LDI-MS) to identify CTCs by analyzing gold cluster ions $[Au_n]^+$ from aptamer-modified gold nanofilms (AuNFs) (Fig. 9b). They found that AuNFs functionalized with mucin1 (MUC1)-binding aptamer (Apt_{MUC1}–AuNFs) could fortify MCF-7 cells selectively from blood samples, and in combination with LDI-MS assessment could permit the specific identification of MCF-7 cells. They could identify as few as 10 MCF-7 cells in samples, using the mentioned Apt_{MUC1}–AuNF/LDI-MS platform. Notably, this Apt_{MUC1}-Au NF/LDI-MS complex operated with no requirement for complex elements (dyes, NPs, or electro-active organic molecules) for tagging destination cells (Chiu et al., 2015).

4. Electrochemical CTCs aptasensors and nano-aptasensors

Electrochemical aptasensors are types of biosensors, which apply an immobilized aptamer on the surface of an electrode for selective attachment to the analyte. This attachment is sensed by an alteration in voltages and/or currents at the localized surface (Ravalli et al., 2016). Electrochemical biosensors are one of the top selected biosensors due to their valuable features including economical operation, multiplexing capabilities (simultaneous analysis of multi-analytes), rapid processing, working with high sensitivity turbid samples, and readily miniaturization capabilities (Golichenari et al., 2019).

Electrochemical biosensors are usually made of two or three electrodes: a chemically stable working (indicator) electrode; a silver-coated reference electrode and an additional platinum wire electrode (Hammond et al., 2016). Various biorecognition elements can be immobilized on an electrode surface in most conventional electrochemical biosensing strategies in order to establish a precise interaction between the

biorecognition element and the target components. The electrical signal from this biointeraction is proportional to the concentration of the target analyte (Ronkainen et al., 2010). Electrochemical biosensors are categorized as voltammetric/amperometric, potentiometric, impedimetric, and conductometric, based on parameters such as electrical current calculation, potential or charge accumulation, impedance, and altered medium conductance, respectively (Golichenari et al., 2019).

Table 4 provides an overview of the LOD and linear range of described electrochemical CTCs nano-aptasensors in the literature.

4.1. Voltammetric/amperometric

Wang group developed an RNA aptamer biochip for both CTCs capture and detection. This polydimethylsiloxane (PDMS) chip included a cover, comprising a channel for the introduction, and maintenance of cells and microelectrode matrix on a silicon dioxide coating. The anti-epidermal growth factor receptor (EGFR) aptamer uniquely binds the cancer cells, enabling the revealing of a single cell by increasing the resistance of ion current between electrodes. This new aptasensor-based strategy was suggested for CTCs isolation from cell counting, peripheral blood, or may be combined with other lab-on-a-chip platforms for follow-up protein and gene analysis (Wang et al., 2012). Qu et al. designed an electrochemical biosensor by simultaneously conjugating two different anti-MEAR cell aptamers, TLS1c and TLS11a, to the surface of a GCE *via* ssDNA and dsDNA, respectively. This biosensor could make it possible for the GCE sensing surface to recognize tumor cells more effectively (Fig. 10a). Experimental results verified the sensitivity improvement of the dual-aptamer modification approach, compared to the single-aptamer modification strategy. In addition, it is possible to exploit other sophisticated signal probes. With a linear range of 1–14 cells, the LOD of the method was one isolated MEAR cell in 10^9 whole blood cells. This work demonstrated a well-designed and ultra-sensitive identification technique, introducing an encouraging possibility for further clinical applications, pertaining to CTCs (Qu et al., 2014).

In another study, an electrochemical-based DNA aptasensor was developed for lung cancer identification. The highly specific aptamer was fixed on a gold microelectrode and electrochemical assessments were carried out in a solution harboring the redox indicator ferrocyanide/ferricyanide. The aptamer/protein targets were collected from the blood of patients *via* streptavidin para-MBs, followed by square wave voltammetry (SWV). In a sandwich detection approach, silica-coated iron oxide MBs with hydrophobic groups were used to improve the sensitivity of the aptasensor. The beads with hydrophobic groups increased the LOD of the aptasensor by 100 times to 0.023 ng mL^{-1}, in the crude blood plasma of subjects with lung cancer (Zamay et al., 2016). Another electrochemical-based strategy is to use an array nanochannel-ionchannel hybrid combined with an electrochemical identification method. In this method, the specific aptamer probe was tied to the surface of ion-channel to specifically capture CTCs. The trapped CTCs effectively cover the entry of the ion channel, which completely blocks the ionic flow *via* the channels, leading to an altered characteristic of the nanochannel-ion channel combination mass transfer property. The captured CTCs can be sensitively identified, by means of an electrochemical linear sweep voltammeter (LSV) method, based on the changed mass transfer properties. Compared to a single channel, the sensitivity of detection can be extremely improved, because of the intensified reaction of array channels. The results showed that the concentration of acute leukemia CCRF-CEM as small as 100 cells mL^{-1} can be captured and detected successfully (Cao et al., 2017).

4.2. Impedance spectroscopy

In 2016, Shen et al. constructed a label-free electrochemical aptasensor with efficient surface identification of EpCAM for CTCs detection based on impedance spectroscopy. In order to achieve the highest sensitivity, after binding of 6-mercapto-1-hexanol (MCH) on the gold electrode, the capture probe was directly pushed in MCH interspaces. The LOD of the aptasensor was 10 cells mL^{-1} with a linear range between 30 to 1×10^6 cells mL^{-1}. The synthesized aptasensor can be reused for 8 times and enriched CTCs can be degraded by Uracil-DNA Excision Mix for further studies (Shen et al., 2016).

Considering the unique properties of the DNA nanotetrahedron (NTH)-based aptamer probe and *in situ* layer-by-layer combination of dendritic structure (DS) nanoprobes, the proposed technique by Sun group significantly improved sensitive and selective electrochemical presentation for examining tumor cells. The target CTCs existing in the sample can challenge DS nanoprobes for binding to NTH-based aptamer probe, which results in the liberation of the DS nanoprobes from the screen-printed gold electrode (SPGE). This method displayed extremely high sensitivity and selectivity toward HepG2 cells with a LOD of five cells mL^{-1}. In addition, their strategy allows the captured cells to be easily detached from the SPGE without negotiating the activity of the cells through an electrochemical breakdown of the Au–S bonds (Sun et al., 2018).

Recently, for the first time, Tian group made an ultrasensitive electrochemical-based aptasensor for the identification of MCF-7 CTCs. In this method, immuno-MBs (Fe_3O_4NPs) were used to both separate and enrich CTCs, and as an enzyme mocks rGO/MoS_2 synergistic catalysis for signal intensification. This aptasensor can simply be regenerated by removing the magnet. The suggested electrochemical aptasensor identified MCF-7 with an LOD of 6 cells mL^{-1} and linearity from 15 to 45 cells mL^{-1} (Tian et al., 2018). In another study, an electrochemical immunosensor for the detection of CTCs was made, using a signal enhancement system based on tyramide signal amplification (TSA). In this method, Pt NPs@HRP complexes and tyramine-functionalized infinite coordination polymers were used to build the TSA-based signal intensification system (Fig. 10b). An improvement was found in the identification of CTCs with a direct concentration, ranging from 2 to 2×10^4 cells mL^{-1} and an acceptable LOD of 2 cells mL^{-1} (Zhou et al., 2019).

4.3. Field-effect transistors (FETs)

Specific sensing with field-effect transistors (FET) biosensor involves integration of bio-recognition elements (e.g. aptamer) with FETs, where the selective interaction between bio-analytes and bio-receptors could lead to biophysical or biochemical changes that can be transduced and amplified *via* field-effect towards external signal readouts. In the case of CTCs detection, recently an incorporated microfluidic chip enriched with FETs sensor arrays coupled with CTC-specific aptamers was developed, which could not only trap CTCs by the chambers narrow necks but also count them through aptamer-based FET sensing. The FET output signal intensity was determined to increase with the growing number of trapped CTCs. In this system, cells could be detached and collected for subsequent applications. This quick identification technique needs just 5-min sample incubation time, which is quicker, in comparison with time-consuming optical imaging techniques (Chen et al., 2019).

However, electrochemical biosensing platforms face several limitations that have been briefly discussed here. Obtained results from electrochemical aptasensors and nanosensors indicate that they are able to detect concentration as small as two cells mL^{-1} of CTCs. It is important to note that CTCs can be identified in trace number in the blood, when cancer is not present, as their level rises in the process of tumor growth. Detection of small CTCs levels is vital for early cancer prognosis screening, and diagnosis, as well as for anticipating the outcome of a particular treatment. Recent techniques do not need a pre-concentration stage, compared to traditional methods and can measure CTCs in very low concentration ranges. Another challenge for the detection of CTCs is the accuracy of cell recognition, as the variety of extended protein structure of the cell membrane increases the complexity of the

recognition. The existence of non-target cells in the model also disrupts the communication of the identification component with the target cells. Accordingly, electrochemical identification of CTCs in human blood with high-sensitivity and high-specificity is a serious concern for non-invasive POC cell identification. Considering this issue, the nano-structured electrode was revealed to elevate the capture efficiency. By using multiplexed cell surface protein profiling, the specificity of the target is enhanced. Likewise, to elevate the specificity of cell identification, the electrochemical assessment of unique metabolic action marker was used on the captured cell. Generally, developing highly specific electrochemical strategies would lead to more accurate cell detection methods implementing POC system.

5. Conclusions and future perspectives

Nowadays, for precise and quick detection of CTCs, aptamer-based biosensors have gained huge attention. With special characteristics including simple synthesis, great diagnostic sensitivity and specificity, and high stability in diverse circumstances, aptamers are one of the most exciting candidates for the construction of sensing platforms. Nevertheless, in spite of several efforts carried out to approve the efficiency of CTCs aptamers in many sensing processes, there is still a long way to propose CTCs aptasensors as a practical technique, regarding the POC diagnostics (Sun et al., 2019).

Most of the platforms reviewed above have only been confirmed, using spiked cells in a diluted buffer or blood sample, which does not represent the exact complexity of real clinical samples. Furthermore, because of the low concentration of these cancer cells in blood, aptasensors detection requires pre-concentration of the clinical specimen. Hence, several milliliters of blood must be processed before detection, and most of the aptasensors-based detection methods have been used for tumor cell detection in PBS or serum solution. Some reviewed platforms are capable of recovering CTCs from a real blood sample, and therefore allow further analysis of the molecular profiling of the captured CTCs at the single cell level. While in some of these platforms, antibodies and peptides were used to target ligands to capture CTCs, the sensitivity, selectivity, and stability of these platforms could be increased by aptamers, leading to an improved chance of success in the clinical applications.

Moreover, in the case of *in vitro* application of aptamers, some practical hurdles, still hinder the development of aptasensors. For instance, large-scale aptamers production is an expensive procedure and aptamers also do not survive sufficiently in blood due to the fast degradation by nucleases. The latter can be addressed by the addition of some functional groups to mimic amino acid side chains in DNA/RNA. A very crucial requirement for the application of almost all above aptamer-based CTCs detection methods is a validation method for distinctions between real samples collected from patients and those prepared in buffer. Additionally, most aptasensors use aptamers with known target proteins, which are not cancer-specific but are existing on the surface of diverse tumor cells. In this regard, the development and evaluation of aptamers for different target cells as well as separate binding sites is needed. In particular, multi-target aptamer-based cytosensors have shown fascinating performance. Consequently, it is very critical to select aptamers with appropriate properties for the target proteins on the surface of tumor cells. For example, MCF-7 cells can be captured more efficiently by using the combination of different aptamers (AS1411, MUC1 and SYL3C) for different biomarkers (EGF, MUC1 and EpCAM).

The integration of NPs with aptasensors in recent years led to reasonable progress in sensitivity and specificity. NPs display unique practical features that often cannot be obtained from either distinct molecules or large size materials. For example, with a large surface-to-volume ratio, NPs can be utilized for greater efficient target communications. This characteristic makes NPs capable of improving the efficiency of the traditional methods and/or to develop novel platforms with enhanced abilities. Nevertheless, for the *in vivo* detection of CTCs, a general concern regarding the biosafety of NPs should be considered. In conclusion, establishing simple, fast, stable, portable, low-cost, and high-performance aptasensors and nano-aptasensors for clinical diagnostics applications of CTCs remains a research trend.

Declaration of competing interest

The authors declare that they have no known competing financial interests or personal relationships that could have appeared to influence the work reported in this paper.

CRediT authorship contribution statement

Hossein Safarpour: Writing - original draft, Writing - review & editing. **Sadegh Dehghani:** Conceptualization. **Rahim Nosrati:** Conceptualization. **Nozhat Zebardast:** Writing - review & editing. **Mona Alibolandi:** Writing - review & editing. **Ahad Mokhtarzadeh:** Funding acquisition, Project administration. **Mohammad Ramezani:** Supervision, Funding acquisition.

Acknowledgments

Foundation for the laboratory of MR is supported by Mashhad University of Medical Sciences, Mashhad, Iran. The authors are grateful for financial support from the Immunology Research Center, Tabriz University of Medical Science, Tabriz, Iran (grant number: 61731).

References

Ali, M.M., Li, F., Zhang, Z., Zhang, K., Kang, D.-K., Ankrum, J.A., Le, X.C., Zhao, W., 2014. Chem. Soc. Rev. 43 (10), 3324–3341.
Aliakbarinodehi, N., Jolly, P., Bhalla, N., Miodek, A., De Micheli, G., Estrela, P., Carrara, S., 2017. Sci. Rep. 7, 44409.
Alix-Panabières, C., Pantel, K., 2014. Nat. Rev. Cancer 14 (9), 623–631.
Anker, J.N., Hall, W.P., Lyandres, O., Shah, N.C., Zhao, J., Van Duyne, R.P., 2008. Nat. Mater. 7 (6), 442–453.
Arya, S.K., Lim, B., Rahman, A.R.A., 2013. Lab Chip 13 (11), 1995–2027.
Bayat, P., Nosrati, R., Alibolandi, M., Rafatpanah, H., Abnous, K., Khedri, M., Ramezani, M., 2018. Biochimie 154, 132–155.
Bhadra, S., Codrea, V., Ellington, A.D., 2014. Anal. Biochem. 445, 38–40.
Bi, S., Hao, S., Li, L., Zhang, S., 2010. Chem. Commun. 46 (33), 6093–6095.
Bi, S., Ji, B., Zhang, Z., Zhang, S.J.C.C., 2013. Chem. Commun. 49 (33), 3452–3454.
Bi, S., Zhou, H., Zhang, S., 2010. Chem. Sci. 1 (6), 681–687.
Bray, F., Ferlay, J., Soerjomataram, I., Siegel, R.L., Torre, L.A., Jemal, A., 2018. CA cancer. J. Clin. 68 (6), 394–424.
Bruno, J., 2015. Molecules 20 (4), 6866–6887.
Cao, J., Zhao, X.-P., Younis, M.R., Li, Z.-Q., Xia, X.-H., Wang, C., 2017. Anal. Chem. 89 (20), 10957–10964.
Cengiz Ozalp, V., Kavruk, M., Dilek, O., Tahir Bayrac, A., 2015. Curr. Top. Med. Chem. 15 (12), 1125–1137.
Chen, G., Qiu, H., Prasad, P.N., Chen, X., 2014. Chem. Rev. 114 (10), 5161–5214.
Chen, K., Liu, B., Yu, B., Zhong, W., Lu, Y., Zhang, J., Liao, J., Liu, J., Pu, Y., Qiu, L., 2017. Wiley Interdiscip. Rev. Nanomed. Nanobiotechnol. 9 (3), e1438.
Chen, M., Bi, S., Jia, X., He, P., 2014. Anal. Chim. Acta 837, 44–51.
Chen, X., Estévez, M.C., Zhu, Z., Huang, Y.-F., Chen, Y., Wang, L., Tan, W., 2009. Anal. Chem. 81 (16), 7009–7014.
Chen, Y.H., Pulikkathodi, A.K., Ma, Y.D., Wang, Y.L., Lee, G.B., 2019. Lab Chip 19 (4), 618–625.
Cheng, L., Yang, K., Zhang, S., Shao, M., Lee, S., Liu, Z., 2010. Nano Res. 3 (10), 722–732.
Chiu, W.-J., Ling, T.-K., Chiang, H.-P., Lin, H.-J., Huang, C.-C., 2015. ACS Appl. Mater. Interfaces 7 (16), 8622–8630.
Cialla, D., Pollok, S., Steinbrücker, C., Weber, K., Popp, J., 2014. Nanophotonics 3 (6), 383–411.
Costa-Fernández, J.M., Pereiro, R., Sanz-Medel, A., 2006. TrAC Trends Anal. Chem. (Reference Ed.) 25 (3), 207–218.
Costa, C., Abal, M., Lopez-Lopez, R., Muinelo-Romay, L., 2014. Sensors 14 (3), 4856–4875.
Cui, F., Ji, J., Sun, J., Wang, J., Wang, H., Zhang, Y., Ding, H., Lu, Y., Xu, D., Sun, X., 2019. Anal. Bioanal. Chem. 411, 1–11.
Damborský, P., Švitel, J., Katrlík, J., 2016. Essays Biochem. 60 (1), 91–100.
Das, P., Sedighi, A., Krull, U., 2018. Anal. Chim. Acta 1041, 1–24.
De Acha, N., Elosua, C., Matias, I., Arregui, F., 2017. Sensors 17 (12), 2826.
Dehghani, S., Nosrati, R., Yousefi, M., Nezami, A., Soltani, F., Taghdisi, S.M., Abnous, K., Alibolandi, M., Ramezani, M., 2018. Biosens. Bioelectron. 110, 23–37.
Dey, D., Goswami, T., 2011. BioMed Res. Int. 2011, 348218.
Dickey, D.D., Giangrande, P.H., 2016. Methods 97, 94–103.

Ding, C., Zhang, C., Yin, X., Cao, X., Cai, M., Xian, Y., 2018. Anal. Chem. 90 (11), 6702–6709.
Dong, H., Gao, W., Yan, F., Ji, H., Ju, H., 2010. Anal. Chem. 82 (13), 5511–5517.
Du, Y., Dong, S., 2017. Anal. Chem. 89 (1), 189–215.
Du, Y.C., Jiang, H.X., Huo, Y.F., Han, G.M., Kong, D.M., 2016. Biosens. Bioelectron. 77, 971–977.
Fang, S., Wang, C., Xiang, J., Cheng, L., Song, X., Xu, L., Peng, R., Liu, Z., 2014. Nano Res. 7 (9), 1327–1336.
Feng, Y., Sun, F., Chen, L., Lei, J., Ju, H., 2016. J. Electroanal. Chem. 781, 48–55.
Gelinas, A.D., Davies, D.R., Janjic, N., 2016. Curr. Opin. Struct. Biol. 36, 122–132.
Golichenari, B., Nosrati, R., Farokhi-Fard, A., Faal Maleki, M., Gheibi Hayat, S.M., Ghazvini, K., Vaziri, F., Behravan, J., 2019. Crit. Rev. Biotechnol. 39 (8), 1056–1077.
Gu, L., Yan, W., Liu, L., Wang, S., Zhang, X., Lyu, M., 2018. Pharmaceuticals 11 (2), 35.
Guan, W., Zhou, W., Lu, J., Lu, C., 2015. Chem. Soc. Rev. 44 (19), 6981–7009.
Guerrini, L., Alvarez-Puebla, R.A., 2019. Cancers 11 (6), 748.
Hammond, J.L., Formisano, N., Estrela, P., Carrara, S., Tkac, J., 2016. Essays Biochem. 60 (1), 69–80.
Hayat, A., Yang, C., Rhouati, A., Marty, J., 2013. Sensors 13 (11), 15187–15208.
Hong, Y., Lee, E., Ku, M., Suh, J.-S., Yoon, D.S., Yang, J., 2016. Nanotechnology 27 (18), 185103.
Hötzer, B., Medintz, I.L., Hildebrandt, N., 2012. Small 8 (15), 2297–2326.
Hutter, E., Maysinger, D., 2013. Trends Pharmacol. Sci. 34 (9), 497–507.
Idris, N.M., Gnanasammandhan, M.K., Zhang, J., Ho, P.C., Mahendran, R., Zhang, Y., 2012. Nat. Med. 18 (10), 1580.
Ignatiadis, M., Lee, M., Jeffrey, S.S., 2015. Clin. Cancer Res. 21 (21), 4786–4800.
Iranifam, M., 2014. TrAC Trends Anal. Chem. (Reference Ed.) 59, 156–183.
Jiang, H.X., Kong, D.M., Shen, H.X., 2014. Biosens. Bioelectron. 55, 133–138.
Jie, G., Wang, L., Yuan, J., Zhang, S., 2011. Anal. Chem. 83 (10), 3873–3880.
Kabashin, A.V., Evans, P., Pastkovsky, S., Hendren, W., Wurtz, G.A., Atkinson, R., Pollard, R., Podolskiy, V.A., Zayats, A.V., 2009. Nat. Mater. 8 (11), 867–871.
Kalinich, M., Bhan, I., Kwan, T.T., Miyamoto, D.T., Javaid, S., LiCausi, J.A., Milner, J.D., Hong, X., Goyal, L., Sil, S., 2017. Proc. Natl. Acad. Sci. U.S.A. 114 (5), 1123–1128.
Karabacak, N.M., Spuhler, P.S., Fachin, F., Lim, E.J., Pai, V., Ozkumur, E., Martel, J.M., Kojic, N., Smith, K., Chen, P.-i., 2014. Nat. Protoc. 9 (3), 694.
Kun, Q., Lin, Y., Peng, H., Cheng, L., Cui, H., Hong, N., Xiong, J., Fan, H., 2018. J. Electroanal. Chem. 808, 101–106.
Kwon, T., Park, J., Lee, G., Nam, K., Huh, Y.-M., Lee, S.-W., Yang, J., Lee, C.Y., Eom, K., 2013. J. Phys. Chem. Lett. 4 (7), 1126–1130.
Li, D., Zhang, Y., Li, R., Guo, J., Wang, C., Tang, C., 2015. Small 11 (18), 2200–2208.
Li, Y., Wu, S., Bai, F., 2018. Semin. Cell Dev. Biol. 75, 88–97.
Li, Y., Zeng, Y., Ji, X., Li, X., Ren, R., 2012. Sens. Actuators B Chem. 171, 361–366.
Li, Z., Wang, G., Shen, Y., Guo, N., Ma, N., 2018. Adv. Funct. Mater. 28 (14), 1707152.
Lin, Y., Jiang, L., Huang, Y., Yang, Y., He, Y., Lu, C., Yang, H., 2019. Chem. Commun. 55 (37), 5387–5390.
Liu, W., Wei, H., Lin, Z., Mao, S., Lin, J.-M.J., 2011. Biosens. Bioelectron. 28 (1), 438–442.
Loh, K.P., Bao, Q., Eda, G., Chhowalla, M., 2010. Nat. Chem. 2 (12), 1015–1024.
Lou, E., Vogel, R.I., Teoh, D., Hoostal, S., Grad, A., Gerber, M., Monu, M., Łukaszewski, T., Deshpande, J., Linden, M.A., 2018. Lab. Med. 49 (2), 134–139.
Malekzad, H., Zangabad, P.S., Mirshekari, H., Karimi, M., Hamblin, M.R., 2017. Nanotechnol. Rev. 6 (3), 301–329.
Malinee, M., Kumar, A., Dhiman, A., Sharma, T.K., 2019. Aptamer-Mediated Nanobiosensing for Health Monitoring. Advanced Biosensors for Health Care Applications. Elsevier, pp. 227–248.
Mansouri, A., Abnous, K., Alibolandi, M., Taghdisi, S.M., Ramezani, M., 2019. J. Cell. Physiol. 234 (10), 18262–18271.
Mayer, G., 2009. Angew. Chem. Int. Ed. 48 (15), 2672–2689.
Medley, C.D., Smith, J.E., Tang, Z., Wu, Y., Bamrungsap, S., Tan, W., 2008. Anal. Chem. 80 (4), 1067–1072.
Mehmood, S., Khan, A., Bilal, M., Sohail, A., Iqbal, H., 2019. Mater. Today Chem. 12, 353–360.
Micalizzi, D.S., Maheswaran, S., Haber, D.A., 2017. Genes Dev. 31 (18), 1827–1840.
Modh, H., Scheper, T., Walter, J.-G., 2018. Sensors 18 (4), 1041.
Mohammadi, S., Salimi, A., Hamd-Ghadareh, S., Fathi, F., Soleimani, F., 2018. Anal. Biochem. 557, 18–26.
Mokhtarzadeh, A., Tabarzad, M., Ranjbari, J., de la Guardia, M., Hejazi, M., Ramezani, M., 2016. TrAC Trends Anal. Chem. (Reference Ed.) 82, 316–327.
Mosafer, J., Abnous, K., Tafaghodi, M., Mokhtarzadeh, A., Ramezani, M., 2017. Eur. J. Pharm. Biopharm. 113, 60–74.
Nam, J.-M., Park, S.-J., Mirkin, C.A., 2002. J. Am. Chem. Soc. 124 (15), 3820–3821.
Nguyen, H.H., Park, J., Kang, S., Kim, M., 2015. Sensors 15 (5), 10481–10510.
Nima, Z.A., Mahmood, M., Xu, Y., Mustafa, T., Watanabe, F., Nedosekin, D.A., Juratli, M. A., Fahmi, T., Galanzha, E.I., Nolan, J.P., Basnakian, A.G., Zharov, V.P., Biris, A.S., 2014. Sci. Rep. 4, 4752.
Norouzi, A., Ravan, H., Mohammadi, A., Hosseinzadeh, E., Norouzi, M., Fozooni, T., 2018. Anal. Chim. Acta 1017, 26–33.
Pandey, P., Datta, M., Malhotra, B., 2008. Anal. Lett. 41 (2), 159–209.
Ping, J., Zhou, Y., Wu, Y., Papper, V., Boujday, S., Marks, R.S., Steele, T.W.J., 2015. Biosens. Bioelectron. 64, 373–385.
Pires, N., Dong, T., Hanke, U., Hoivik, N., 2014. Sensors 14 (8), 15458–15479.
Qu, L., Xu, J., Tan, X., Liu, Z., Xu, L., Peng, R., 2014. ACS Appl. Mater. Interfaces 6 (10), 7309–7315.
Ranc, V., Srovnal, J., Kvítek, L., Hajduch, M., 2013. Analyst 138 (20), 5983–5988.
Ravalli, A., Voccia, D., Palchetti, I., Marrazza, G., 2016. Biosensors 6 (3), 39.
Roda, A., Mirasoli, M., Michelini, E., Di Fusco, M., Zangheri, M., Cevenini, L., Roda, B., Simoni, P., 2016. Biosens. Bioelectron. 76, 164–179.
Ronkainen, N.J., Halsall, H.B., Heineman, W.R., 2010. Chem. Soc. Rev. 39 (5), 1747–1763.
Scheller, F.W., Yarman, A., Bachmann, T., Hirsch, T., Kubick, S., Renneberg, R., Schumacher, S., Wollenberger, U., Teller, C., Bier, F.F., 2014. Adv. Biochem. Eng. Biotechnol. 140, 1–28.
Schettini, F., Giuliano, M., Cristofanilli, M., 2019. Chapter 12 - prognostic and predictive role of circulating tumor cells. In: Dammacco, F., Silvestris, F. (Eds.), Oncogenomics. Academic Press, pp. 181–190.
Sha, M.Y., Xu, H., Natan, M.J., Cromer, R., 2008. J. Am. Chem. Soc. 130 (51), 17214–17215.
Shen, H., Yang, J., Chen, Z., Chen, X., Wang, L., Hu, J., Ji, F., Xie, G., Feng, W., 2016. Biosens. Bioelectron. 81, 495–502.
Shen, Z., Wu, A., Chen, X., 2017. Chem. Soc. Rev. 46 (8), 2038–2056.
Shi, H., Li, D., Xu, F., He, X., Wang, K., Ye, X., Tang, J., He, C., 2014. Analyst 139 (17), 4181–4184.
Shi, W., Paproski, R.J., Moore, R., Zemp, R., 2014. J. Biomed. Opt. 19 (5), 056014.
Siegel, R.L., Miller, K.D., Jemal, A., 2018. CA cancer. J. Clin. 68 (1), 7–30.
Šípová, H., Homola, J., 2013. Anal. Chim. Acta 773, 9–23.
Smith, R.A., Andrews, K.S., Brooks, D., Fedewa, S.A., Manassaram-Baptiste, D., Saslow, D., Brawley, O.W., Wender, R.C., 2018. CA cancer. J. Clin. 68 (4), 297–316.
Song, K.M., Lee, S., Ban, C., 2012. Sensors 12 (1), 612–631.
Song, Y., Zhu, Z., An, Y., Zhang, W., Zhang, H., Liu, D., Yu, C., Duan, W., Yang, C.J., 2013. Anal. Chem. 85 (8), 4141–4149.
Sriramoju, B., Kanwar, R., N Veedu, R., R Kanwar, J., 2015. Curr. Top. Med. Chem. 15 (12), 1115–1124.
Sun, C., Zhang, R., Gao, M., Zhang, X., 2015. Anal. Bioanal. Chem. 407 (29), 8883–8892.
Sun, D., Lu, J., Chen, D., Jiang, Y., Wang, Z., Qin, W., Yu, Y., Chen, Z., Zhang, Y., 2018. Sens. Actuators B Chem. 268, 359–367.
Sun, D., Lu, J., Zhang, L., Chen, Z., 2019, 1-17. Anal. Chim. Acta. ***1082***,.
Sundling, K.E., Lowe, A.C., 2019. Adv. Anat. Pathol. 26 (1), 56–63.
Szeto, K., Latulippe, D.R., Ozer, A., Pagano, J.M., White, B.S., Shalloway, D., Lis, J.T., Craighead, H.G., 2013. PLoS One 8 (12), e82667.
Szunerits, S., Boukherroub, R., 2018. Interface focus 8 (3), 20160132.
Tang, L., Liu, Y., Ali, M.M., Kang, D.K., Zhao, W., Li, J., 2012. Anal. Chem. 84 (11), 4711–4717.
Tian, L., Qi, J., Qian, K., Oderinde, O., Cai, Y., Yao, C., Song, W., Wang, Y., 2018. Sens. Actuators B Chem. 260, 676–684.
Ukaegbu, M., Enwerem, N., Bakare, O., Sam, V., Southerland, W., Vivoni, A., Hosten, C., 2016. J. Mol. Struct. 1114, 197–205.
Vigneshvar, S., Sudhakumari, C., Senthilkumaran, B., Prakash, H., 2016. Front. Bioeng. Biotechnol. 4, 11.
Viraka Nellore, B.P., Kanchanapally, R., Pramanik, A., Sinha, S.S., Chavva, S.R., Hamme, A., Ray, P.C., 2015. Bioconjug. Chem. 26 (2), 235–242.
Vorobyeva, M., Davydova, A., Vorobjev, P., Pyshnyi, D., Venyaminova, A., 2018. ?Int. J. Mol. Sci. 19 (2), 470.
Wang, C., Cheng, L., Liu, Z., 2011. Biomaterials 32 (4), 1110–1120.
Wang, J., Dong, H.-y., Zhou, Y., Han, L.-y., Zhang, T., Lin, M., Wang, C., Xu, H., Wu, Z.-S., Jia, L., 2018. Biosens. Bioelectron. 122, 239–246.
Wang, K., Fan, D., Liu, Y., Wang, E., 2015. Biosens. Bioelectron. 73, 1–6.
Wang, L., Zheng, Q., Zhang, Q.a., Xu, H., Tong, J., Zhu, C., Wan, Y., 2012. Oncol. Lett. 4 (5), 935–940.
Wang, X., Qian, X., Beitler, J.J., Chen, Z., Khuri, F.R., Lewis, M.M., Shin, H.J., Nie, S., Shin, D.M., 2013. Cancer Res. 73 (8 Supplement), 1460-1460.
Wang, Y., Li, Z., Hu, D., Lin, C.T., Li, J., Lin, Y., 2010. J. Am. Chem. Soc. 132 (27), 9274–9276.
Wang, Z., Qin, W., Zhuang, J., Wu, M., Li, Q., Fan, C., Zhang, Y., 2019. ACS Appl. Mater. Interfaces 11 (13), 12244–12252.
Wen, S., Zhou, J., Zheng, K., Bednarkiewicz, A., Liu, X., Jin, D., 2018. Nat. Commun. 9 (1), 2415.
Wijaya, E., Lenaerts, C., Maricot, S., Hastanin, J., Habraken, S., Vilcot, J.P., Boukherroub, R., Szunerits, S., 2011. Curr. Opin. Solid State Mater. Sci. 15 (5), 208–224.
Wilhelm, S., 2017. ACS Nano 11 (11), 10644–10653.
Wu, L., Ma, C., Ge, L., Kong, Q., Yan, M., Ge, S., Yu, J., 2015. Biosens. Bioelectron. 63, 450–457.
Wu, X., Luo, L., Yang, S., Ma, X., Li, Y., Dong, C., Tian, Y., Zhang, L.e., Shen, Z., Wu, A., 2015. ACS Appl. Mater. Interfaces 7 (18), 9965–9971.
Xiang, D., Shigdar, S., Qiao, G., Wang, T., Kouzani, A.Z., Zhou, S.-F., Kong, L., Li, Y., Pu, C., Duan, W., 2015. Theranostics 5 (1), 23.
Xu, L., Jiang, Z., Mu, Y., Zhang, Y., Zhan, Q., Cui, J., Cheng, W., Ding, S., 2018. Sens. Actuators B Chem. 259, 596–603.
Yang, Y., 2014. Microchim. Acta 181 (3–4), 263–294.
Yao, C., Cheng, F., Wang, C., Wang, Y., Guo, X., Gong, Z., Fan, M., Zhang, Z., 2013. Anal. Methods 5 (20), 5560–5564.
Yazdian-Robati, R., Arab, A., Ramezani, M., Rafatpanah, H., Bahreyni, A., Nabavinia, M. S., Abnous, K., Taghdisi, S.M., 2019. Drug Dev. Ind. Pharm. 45 (4), 603–610.
Yoo, S.M., Lee, S.Y., 2016. Trends Biotechnol. 34 (1), 7–25.
Zamay, G.S., Kolovskaya, O.S., Zamay, T.N., Glazyrin, Y.E., Krat, A.V., Zubkova, O., Spivak, E., Wehbe, M., Gargaun, A., Muharemagic, D., 2015. Mol. Ther. 23 (9), 1486–1496.
Zamay, G.S., Zamay, T.N., Kolovskii, V.A., Shabanov, A.V., Glazyrin, Y.E., Veprintsev, D. V., Krat, A.V., Zamay, S.S., Kolovskaya, O.S., Gargaun, A., 2016. Sci. Rep. 6, 34350.
Zeng, Z., Tung, C.-H., Zu, Y., 2014. Mol. Ther. Nucleic Acids 3, e184.
Zhang, P., Zhang, R., Gao, M., Zhang, X., 2014. ACS Appl. Mater. Interfaces 6 (1), 370–376.

Zhang, X., Hu, Y., Yang, X., Tang, Y., Han, S., Kang, A., Deng, H., Chi, Y., Zhu, D., Lu, Y., 2019. Biosens. Bioelectron. 138, 111314.
Zhang, Y., Lai, B.S., Juhas, M., 2019. Molecules 24 (5), 941.
Zhang, Y., Wang, Z., Wu, L., Zong, S., Yun, B., Cui, Y., 2018. Small 14 (20), 1704433.
Zhang, Y., Zhao, S., Zheng, J., He, L., 2017. TrAC Trends Anal. Chem. (Reference Ed.) 90, 1–13.
Zhao, W., Ali, M.M., Brook, M.A., Li, Y., 2008. Angew. Chem. Int. Ed. 47 (34), 6330–6337.
Zheng, F., Cheng, Y., Wang, J., Lu, J., Zhang, B., Zhao, Y., Gu, Z., 2014. Adv. Mater. 26 (43), 7333–7338.
Zhou, J., Rossi, J., 2017. Nat. Rev. Drug Discov. 16 (3), 181.
Zhou, X., Li, Y., Wu, H., Huang, W., Ju, H., Ding, S., 2019. Biosens. Bioelectron. 130, 88–94.
Zhou, Y., Mahapatra, C., Chen, H., Peng, X., Ramakrishna, S., Nanda, H.S., 2020. Curr. Opin. Biomed. Eng. 13, 16–24.